JEM Journal of Experimental Medicine

ARTICLE

JNK1 inhibitors target distal B cell receptor signaling and overcome BTK-inhibitor resistance in CLL

Shifa Khaja Saleem[1], Sarah Decker[1], Sandra Kissel[1], Marcus Bauer[2], Dmitry Chernyakov[3], Daniela Bräuer-Hartmann[3], Konrad Aumann[4], Claudia Wickenhauser[2], Marco Herling[5], Oleksandra Skorobohatko[3], Nimitha Mathew[1], Cornelius Schmidt[1], Claudius Klein[1,6], Marie Follo[1], and Christine Dierks[1,3]

Inhibition of the proximal B cell receptor (BCR) signaling pathway by BTK inhibitors is highly effective in the treatment of CLL, but drug resistance or intolerance occurs. Here, we investigated c-Jun N-terminal protein kinase 1 (JNK1) as an alternative drug target in the distal BCR pathway. JNK1 was preferentially overexpressed and activated in poor prognostic CLL with unmutated IGHV. Proximal BCR inhibition (BTK, PI3K, or SYK inhibitors) or SYK knockdown efficiently dephosphorylated JNK1, identifying JNK1 as a critical BCR downstream kinase in CLL. JNK1 inhibition induced apoptosis in primary CLL cells, resulting in the downregulation of BCL2, MCL1, and c-JUN. JNK1 inhibition in patient-derived CLL xenografted mice and Eμ-TCL1-tg mice prevented CLL progression, reduced splenic infiltration, and restored T cell function and normal hematopoiesis. JNK1 inhibitors even remained effective in ibrutinib refractory CLL. In conclusion, our study revealed JNK1 as a promising drug target in CLL downstream of the BCR, overcoming ibrutinib resistance, blocking the protective microenvironment, and improving CLL-specific immunosuppressive mechanisms.

Introduction

Chronic lymphocytic leukemia (CLL) is the most prevalent leukemia in elderly patients and is characterized by an uncontrolled expansion of clonal B cells in peripheral blood (PB), bone marrow (BM), lymph nodes, and spleen resulting in splenomegaly, lymphadenopathy, and repression of normal hematopoietic cells in the BM. This results in progressive anemia and thrombocytopenia as well as immunoglobulin deficiency and an additional imbalance within the T cell compartment toward an immunosuppressive environment (Ghia and Caligaris-Cappio, 2006; Chiorazzi et al., 2005). Prognostic markers such as Rai and Binet staging systems, ζ-associated protein 70 (ZAP70) expression (Rassenti et al., 2004; Wiestner et al., 2003), cytogenetic abnormalities (Hallek et al., 2008), immunoglobulin variable heavy chain (IGHV), and other gene mutations can be used to predict survival outcome and guide treatment choices in patients with CLL (Landau et al., 2013; Puente et al., 2011).

Major disease drivers in CLL involve the constitutive activation of the B cell receptor (BCR) pathway, as well as additional antiapoptotic pathways resulting in B cell lymphoma 2 (BCL2) overexpression and activation. Constitutive BCR signaling in CLL can be induced by the recognition of internal BCR epitopes (Dühren-von Minden et al., 2012; Minici et al., 2017) or by the recognition of antigens outside the CLL cells within the CLL microenvironment (Burger and Chiorazzi, 2013; Chen et al., 2013; Binder et al., 2010). CLL patients with an unmutated IGHV status have more polyreactive BCRs and a higher degree of BCR activation compared with IGHV mutated CLLs and demonstrate a more aggressive disease phenotype with shorter survival and a more frequent need for treatment (Hamblin et al., 1999; Hervé et al., 2005; Agathangelidis et al., 2012). Pharmacological inhibition of BCR proximal kinases like Brutons's tyrosin kinase (BTK), spleen tyrosin kinase (SYK), or phosphoinositide 3-kinase (PI3K) can therefore be used to block CLL cell survival, proliferation, and migration (Herman et al., 2014; Morabito et al., 2015).

Ibrutinib, a first-in-class BTK inhibitor, has demonstrated high response rates in both relapsed/refractory and treatment-naive CLL (Burger et al., 2015; Byrd et al., 2013), and BTK inhibitors as well as BCL2 inhibitors like venetoclax are now used as first-line options for CLL treatment. Despite its great clinical

[1]Department of Hematology and Oncology, Freiburg University Medical Center, Albert-Ludwigs-University of Freiburg, Breisgau, Germany; [2]Institute of Pathology, University Hospital Halle, Martin Luther University Halle-Wittenberg, Halle, Germany; [3]Department of Hematology/Oncology and Stem Cell Transplantation, KIM IV, Martin-Luther University Halle-Wittenberg, Halle, Germany; [4]Department of Pathology, Freiburg University Medical Center, Albert-Ludwigs-University of Freiburg, Breisgau, Germany; [5]Department of Hematology, Cellular Therapy, Hemostaseology and Infectious Diseases, University of Leipzig, Leipzig, Germany; [6]Department of Nuclear Medicine, Freiburg University Medical Center, Albert-Ludwigs-University of Freiburg, Breisgau, Germany.

Correspondence to Christine Dierks: christine.dierks@uk-halle.de.

activity, about 25% of ibrutinib-treated patients stopped ibrutinib at a median follow-up of 20 mo due to treatment resistance/relapse (40–42%) or side effects. Treatment resistance was defined as leukemia progression, but about half of the patients even developed Richter's transformation. For these patients, treatment options are limited and outcomes are dismal with a mortality rate of >75% within 1 year and a median overall survival of 3 mo (Maddocks et al., 2015; Jain et al., 2017).

C-Jun N-terminal protein kinase 1 (JNK1) is a member of the mitogen-activated protein kinase (MAPK) superfamily, which also includes the extracellular signal-regulated kinase (ERK) and the p38 family of kinases (Hibi et al., 1993). JNK includes three isoforms (JNK1, JNK2, and JNK3). JNK1 and JNK2 are ubiquitously expressed whereas JNK3 expression is restricted to the brain, heart, and testes. JNK proteins are also known as stress-activated protein kinases (SAPKs), activated via phosphorylation in response to various stimuli such as cytokines, stress, and growth factors (Davis, 2000; Weston and Davis, 2007). The serine–threonine kinase JNK1 is involved in cell proliferation, survival, differentiation, and apoptosis dependent on the cellular context. Activated JNK1 phosphorylates transcription factors such as c-JUN, c-MYC, ELK1, p53, NFAT, STAT1, and STAT3 as well as members of the BCL2 family such as BCL2, BCL-XL, and MCL-1 (Bogoyevitch and Kobe, 2006; Lin, 2003; Yu et al., 2004). JNK1 activity is required in BCR-ABL–mediated transformation of pre-B cells in vitro and in vivo (Hess et al., 2002). Furthermore, JNK1 is activated in acute myeloid leukemia with active FLT3 signaling and T cell acute lymphoblastic leukemia (Hartman et al., 2006). JNK1 inhibition with small molecule inhibitors or siRNA-mediated JNK1 knockdown reduces tumor growth, induces cell cycle arrest and apoptosis in ovarian cell carcinoma, prostate cancer, and melanoma (Vivas-Mejia et al., 2010; Alexaki et al., 2008; Parra, 2012).

Our study focused on the role of JNK1 as a crucial signaling mediator of BCR signaling and as a therapeutic target in bad prognostic and ibrutinib/BTK-inhibitor-refractory CLL.

Results

JNK1 is overexpressed and hyperphosphorylated in primary human CLL cells

In this project, we aimed to identify kinases overexpressed and activated in CLL, which might be potential therapeutic targets for this disease. First, we analyzed gene expression studies (RNA sequencing/Affimetrix gene arrays) published from different groups in the GEO database that compared CLL patient samples with normal B cells and identified MAPK8/JNK1 to be overexpressed in different CLL datasets (GDS3902, GDS4168; Fig. 1, A and B) (Vargova et al., 2011; Gutierrez et al., 2010). This finding could be reconfirmed in our own patient cohort by quantitative PCR, and we found a significant 3.5-fold increase of JNK1 mRNA levels in CLL samples (n = 20) compared with CD19$^+$ normal B lymphocytes from healthy donors (n = 7) (Fig. 1 C; individual values in Table S2). Immunoblots for total and phosphorylated JNK1 protein expression revealed a significant overexpression and phosphorylation of JNK1 in the majority of CLLs (20/21) despite distinct genetic aberrations, while JNK1 protein was absent in normal CD19$^+$ B lymphocytes from healthy donors (n = 7) (Fig. 1 D shows 2 healthy controls and 12 CLL samples). In contrast to JNK1, both JNK2 and JNK3 were not overexpressed in CLL (RNA levels) and were not hyperphosphorylated (data not shown). The JNK1 phosphorylation levels were significantly higher in IGHV unmutated CLL patient samples (n = 8) compared with IGHV mutated CLL patient samples (n = 13) (Fig. 1 G), which already associates JNK1 phosphorylation with BCR signaling (individual data in Table S2). To confirm our results, we then performed immunohistochemistry (IHC) staining for JNK1 in lymph nodes from patients with reactive enlarged lymph nodes (n = 21) and from CLL patients (n = 28) (Fig. 1 J). JNK1 was significantly more expressed in lymph nodes from CLL patients compared with reactive lymph nodes, where it was exclusively expressed in germinal centers, which contain the activated, proliferative B cell population (Fig. 1, H–J). JNK1 phosphorylation was detectable at low levels by IHC and was exclusively present in lymph nodes from CLL patients (Fig. 1, I and J). Our data confirm that JNK1 is overexpressed and hyperphosphorylated in CLL, with the strongest phosphorylation present in IGHV unmutated CLL samples.

JNK1 knockdown and JNK1 inhibition induce apoptosis in primary CLL cells with preferentially unmutated IGHV and poor prognosis

To further elucidate the role of JNK1 in CLL, we performed JNK1 knockdown experiments in primary CLLs (n = 4) with four different siRNAs against JNK1 using the Amaxa Biosystems Nucleofector II (Fig. 2 A) knockdown technology. siRNA-mediated JNK1 knockdown (kd) was achieved with all four siRNAs and reduced JNK1 expression levels between 20% and 80%. JNK1 kd induced apoptosis between 25% and 43% in primary CLL cells compared with the non-silencing control (Fig. 2 B). Apoptosis induction correlated with knockdown efficiency (Fig. 2 C). Next, JNK1 was inhibited with three different JNK1 inhibitors (Fig. 2 D), which had been previously used in other cancer entities (Cui et al., 2009; Grassi et al., 2015). L-JNKi is an inhibitory peptide designed against the binding sequence of JNK1 and prevents the binding of JNK1 to its substrates. The JNK1 kinase inhibitors SP600125 and CC-930 are ATP-competitive kinase inhibitors and inhibit substrate phosphorylation. In primary CLL cells (n = 43), JNK1 inhibitor treatment with SP600125, CC-930, and L-JNKi resulted in apoptosis induction (>30% after 24 h) in the majority of samples, but some samples were also primary resistant (Fig. 2 E). In contrast to CLL, JNK1 inhibition did not affect the survival of normal CD19$^+$ B cells from healthy donors (n = 5) even in the highest concentration (Fig. 2 F and Fig. S1). Treatment response in CLL was quantified at 24 h according to apoptosis induction at the 2.5 µM inhibitor concentration compared with control (sensitive if >30% apoptosis induction) and according to half-maximal inhibitory concentration (IC50) values (<2.5 µM with kinase inhibitors, <5 µM with L-JNKi). Response groups were defined as JNK1-inhibitor responsive if the CLL sample responded to all three inhibitors, intermediate responsive (sensitive to one to two inhibitors), and resistant (no response to any inhibitor). According to apoptosis measurements, 49% of the samples were responsive, 30% intermediate

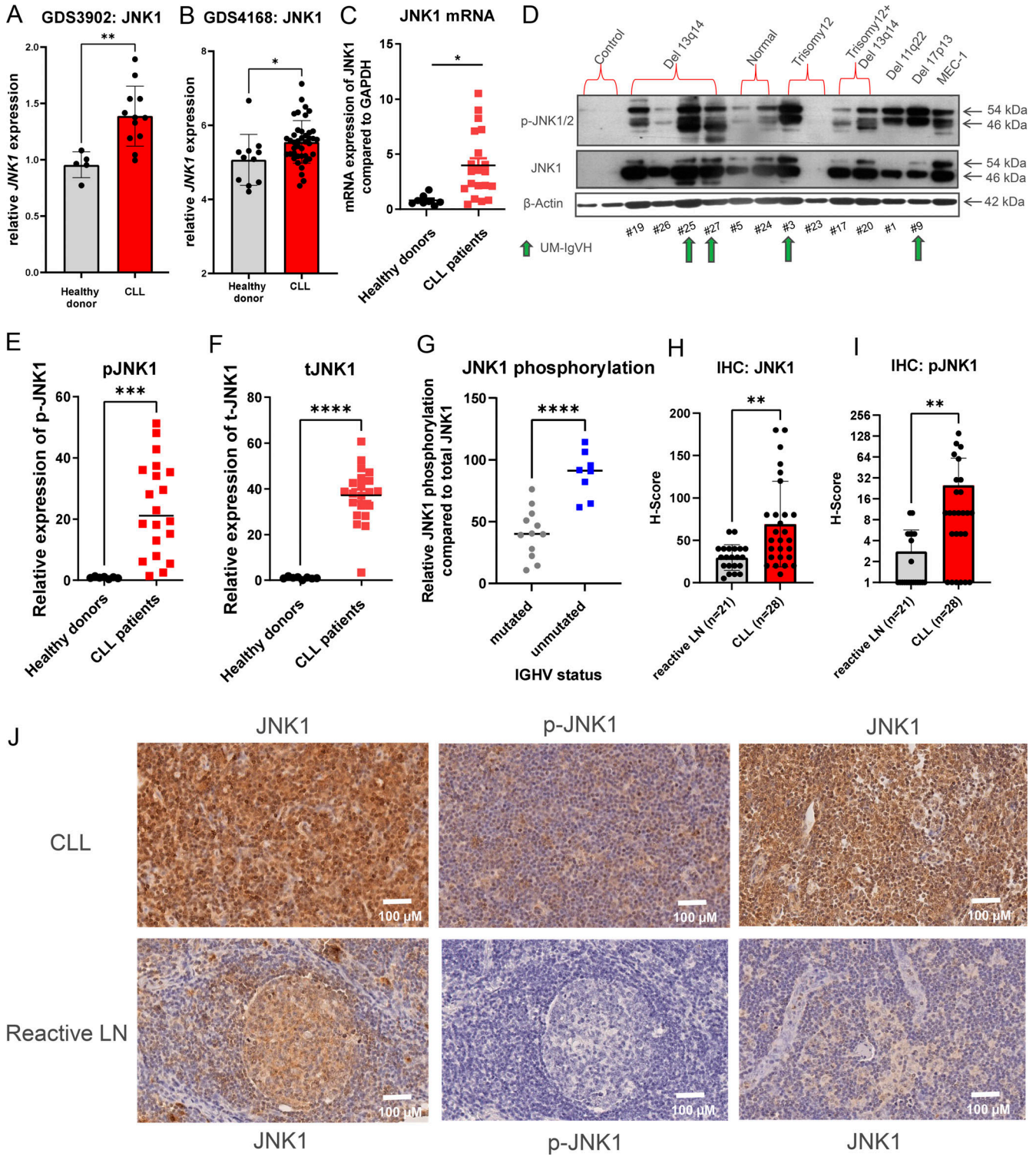

Figure 1. **JNK1 is overexpressed and hyperphosphorylated in primary human CLL. (A and B)** Gene sets, GDS3902 (n = 16) and GDS4168 (n = 36) published in the GEO database comparing B cells from healthy donors with CLLs were analyzed regarding JNK1 mRNA expression (unpaired t test, *P < 0.05; **P < 0.01). **(C)** TaqMan PCR was performed for JNK1 and GAPDH from RNA extracted from CLL patient samples (n = 20, patients #1–20) and CD19⁺ lymphocytes from healthy donors (n = 7). JNK1 transcript levels were normalized to GAPDH and healthy donor control was set to 1 (patient characteristics in Table S1; unpaired t test, *P < 0.05). **(D)** Protein expression of p-JNK1 and total JNK1 in CLL patient samples (n = 12), and CD19⁺ lymphocytes from healthy donors (n = 2). β-Actin was used as a loading control and MEC1 cells as a positive control. Patients with unmutated IGHV are marked with green arrows. **(E and F)** Relative expression of p-JNK1 and total JNK1 were compared with β-actin in CLL patient samples (n = 21) and CD19⁺ lymphocytes from healthy donors (n = 7 controls). Western blots: Fig. 1 D and data not shown (unpaired t test, ***P < 0.001, ****P < 0.0001). **(G)** Relative phospho-JNK1 compared with total JNK1 in IGHV mutated (n = 13) and unmutated (n = 8) CLL patient samples (unpaired t test, ****P < 0.0001). **(H)** JNK1 level (H-score) in reactive lymph nodes (n = 21) and lymph nodes from CLL patients (n = 28) (unpaired t test, **P < 0.01). **(I)** Phospho-JNK1 levels in the same samples (unpaired t test, **P < 0.01). **(J)** Representative examples of IHC images from lymph nodes of CLL patients (upper row) or reactive lymph nodes (lower row) stained for total JNK1 (first and last column) or phospho-JNK1 (medium column). Source data are available for this figure: SourceData F1.

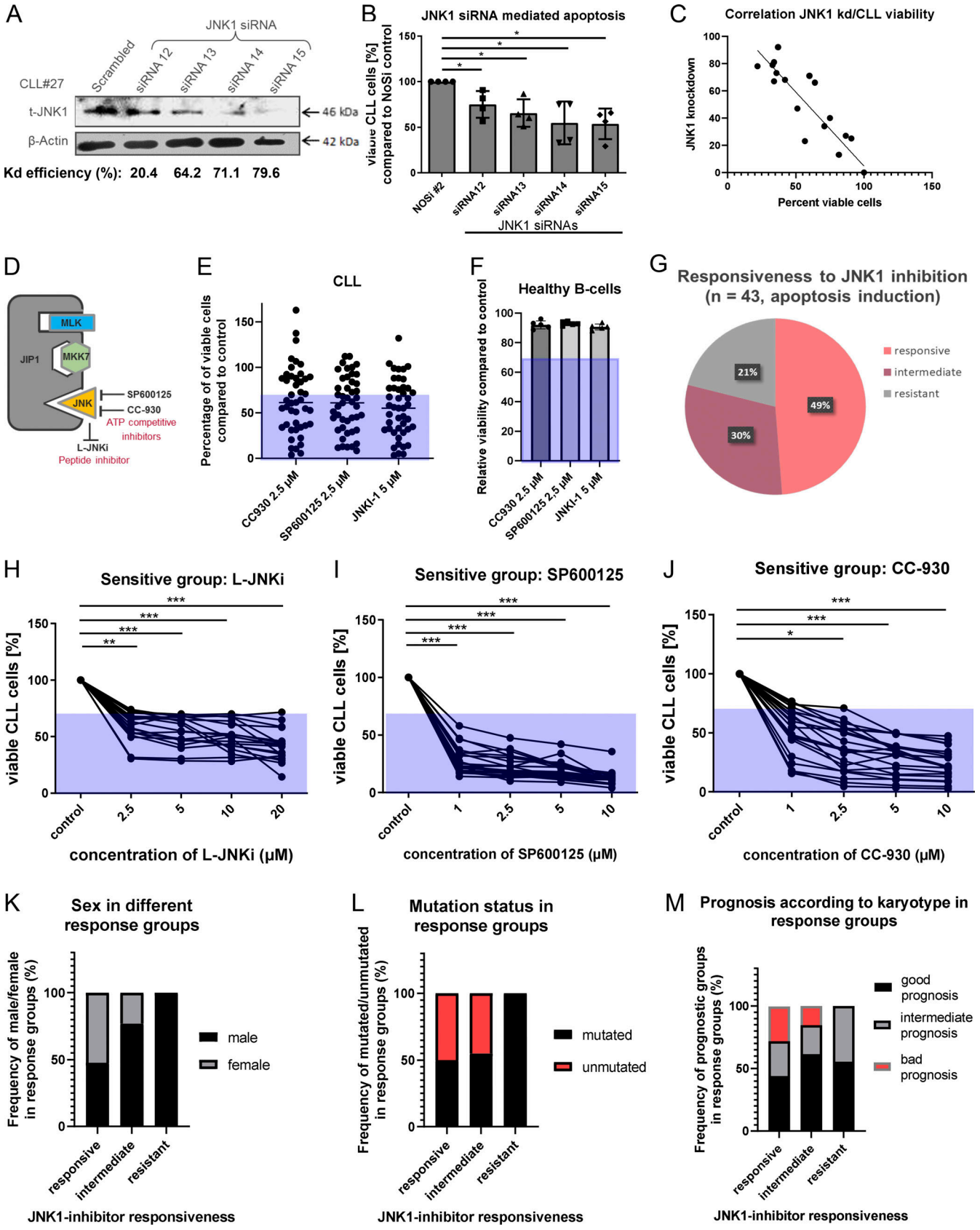

Figure 2. **JNK1 knockdown and JNK1 inhibition induces apoptosis in primary human CLL cells. (A)** Knockdown efficiency in CLL patient samples using four different JNK1-siRNAs for 24 h (CLL#27; figure shows one out of four patient samples). **(B)** Viable CLL cells after 36 h of JNK1 knockdown using four different siRNAs (n = 4) in four different CLLs. Bar shows the mean viability for all four CLL patients (unpaired t test, *P < 0.05). **(C)** Correlation of JNK1 kd

efficiency (A) with CLL cell viability (B). **(D)** Mechanism of action of the ATP-competitive JNK1 inhibitors SP600125 and CC-930 and the L-JNKi inhibitory peptide. **(E)** Relative amount of viable CLL cells treated with the three different JNK1 inhibitors at the indicated concentrations compared with DMSO control (n = 43 CLLs). **(F)** Relative amount of viable B cells from healthy donors after treatment with three JNK1 inhibitors at indicated concentrations compared to DMSO control (n = 5). **(G)** Response groups according to apoptosis induction after JNK1 inhibitor treatments with three different JNK1 inhibitors in 43 CLL patient samples. Sensitivity to one inhibitor was defined as relative apoptosis induction of >30% with the 2.5 µM inhibitor concentration (kinase inhibitors) and the 5 µM concentration (JNK1i) compared with control treatment. Responsive was defined as a CLL sample, which responded to all three inhibitors, intermediate responsive samples responded to one to two inhibitors and resistant samples did not respond to any inhibitor. **(H–J)** Quantification of relative viable CLL cells treated with three different JNK1 inhibitors for 24 h compared with controls, here showing all samples in the responsive group, which are sensitive to all three inhibitors (n = 21) (unpaired t test, *P < 0.05, **P < 0.01, ***P < 0.001). **(K–M)** Distribution of patient characteristics like sex, mutation status (IGHV mutated or unmutated), or prognosis according to karyotype and p53 status (complex karyotype, 11q-, 17p-, or p53 mutation) within the different response groups. Source data are available for this figure: SourceData F2.

responsive, and 21% resistant to JNK1 inhibition (Fig. 2 G). Similar results were obtained with IC50 criteria (45% responsive, 31% intermediate responsive, and 24% resistant) (Fig. S2). Response to all three inhibitors was dose dependent (Fig. 2, H–J shows the 21 CLL samples from the responsive group for all three inhibitors), and responsiveness to one inhibitor was positively correlated with responsiveness to any of the other two inhibitors. Treatment resistance was associated with mutated IGHV and male sex (Fig. 2, K and L). Unfavorable parameters, like complex karyotype, 17p deletion, 11q deletion, or unmutated IGHV status were all in the JNK1 inhibitor sensitive or intermediate group (Fig. 2, L and M), defining JNK1 as an interesting target for these unfavorable prognostic patient subsets.

JNK1 inhibition affects BCL2 and MCL1 expression in CLL

Previous studies in ALL and solid tumors have shown that activated JNK1 phosphorylates members of the BCL2 family such as BCL2 and MCL1. BCL2 is highly expressed in CLL cells, and BCL2 inhibitors (venetoclax) are effective treatment options for CLL. MCL1 expression correlates with bad prognostic factors in CLL such as stage of disease, lymphocyte doubling time, IGHV unmutated status, ZAP-70, and CD38 expression in CLL (Pepper et al., 2008). Primary CLL cells were treated with the two different JNK1 kinase inhibitors SP600125 and CC-930 or the inhibitory peptide L-JNKi and immunoblots were performed for phosphorylated and total JNK1, phosphorylated and total BCL2, and phosphorylated and total MCL1. Both JNK1 kinase inhibitors induced dephosphorylation of JNK1 within 4 h, while total JNK1 levels were not significantly changed (t-JNK1) (Fig. 3, A and E). Furthermore, phosphorylation and also total protein levels of BCL2 and MCL1 were reduced (Fig. 3, C and E). As expected, the L-JNKi inhibitory peptide, which inhibits substrate binding to JNK1 did not alter total JNK1 expression or JNK1 phosphorylation (Fig. 3, B and E), but efficiently reduced BCL2 and MCL1 phosphorylation within 4 h (Fig. 3, D and E). In addition, kd of JNK1 with two different siRNAs also reduced phosphorylated and total BCL2 levels within 24 h (Fig. 3, F and G).

JNK1 inhibition reduces CLL cell viability preferentially in IGHV unmutated CLLs and overcomes stromal protective effects

The microenvironment including stromal cells, nurse-like cells, and T cells plays an important role in disease progression and drug resistance of CLL (Burger et al., 2000). This can be partially recapitulated in vitro by the co-cultivation of CLL cells with the stromal cell line M2-10B4 (Burroughs et al., 1994), which secretes CXCL12 and other CLL-supporting cytokines, or the CD40 ligand–producing cell line, which mimics T cell interaction (van Attekum et al., 2017). IGHV unmutated (n = 11) and mutated (n = 12) CLL samples were cocultured with both cell lines and treated with the JNK1 inhibitor SP60012. As expected, IGHV unmutated CLL samples strongly responded to JNK1 inhibition with a dose-dependent reduction in CLL viability (Fig. 4 A), while CLLs with mutated IGHV status were less sensitive (Fig. 4 B). The co-cultivation of CLL cells with M2-10B4 cells or CD40 ligand–producing cells strongly enhanced the number of viable CLL cells in the control groups. Nevertheless, co-culture did not affect the responsiveness of IGHV unmutated patient samples to JNK1 inhibition (Fig. 4 A), and could even partially overcome stroma-protective effects in IGHV mutated patient samples (Fig. 4 B).

Next, we investigated the effect of M2-10B4/CD40L stroma co-culture on JNK1 activation in CLL cells. Interestingly, co-culture further induced JNK1 phosphorylation in CLL cells (Fig. 4, C and D). JNK1 inhibitor treatment with SP600125 could fully inhibit stroma-induced JNK1 phosphorylation (Fig. 4, C and D) and block the phosphorylation of its downstream targets MCL1, BCL2, and the oncogenic transcription factor c-JUN (Fig. 4, E and F). While JNK1 inhibitors reduced the viability of CLL cells, they had no effect on apoptosis or proliferation of M2-10B4 cells or CD40L-producing cells (Fig. S3). Our results indicate that stromal cells can activate and phosphorylate JNK1 in CLL cells, but JNK1 inhibitors effectively induce apoptosis via downregulation of BCL2 and MCL1 even in microenvironmentally stimulated and protected CLL cells.

JNK1 is a crucial downstream mediator of BCR signaling in CLL

Due to the fact that IGHV unmutated CLLs with a higher BCR activation level have a higher JNK1 phosphorylation (Fig. 1) and are more responsive to JNK1 inhibitors (Fig. 4 A), we hypothesized that JNK1 is involved in BCR signaling in CLL. To prove this, we inhibited three different proximal BCR kinases by using the SYK inhibitor entospletinib, the BTK inhibitor ibrutinib, and the PI3K inhibitor idelalisib. All three upstream BCR inhibitors reduced the phosphorylation of their specific target kinase in CLL cells (Fig. 5 A, first lane). Furthermore, the inhibition of any of those upstream kinases all induced dephosphorylation of JNK1 within 4 h of treatment, while total JNK1 levels were unaffected. This effect could be recapitulated and quantified in several primary CLL samples (n = 4) and shows the strongest effects on JNK1 dephosphorylation for the BTK inhibitor ibrutinib (Fig. 5, A

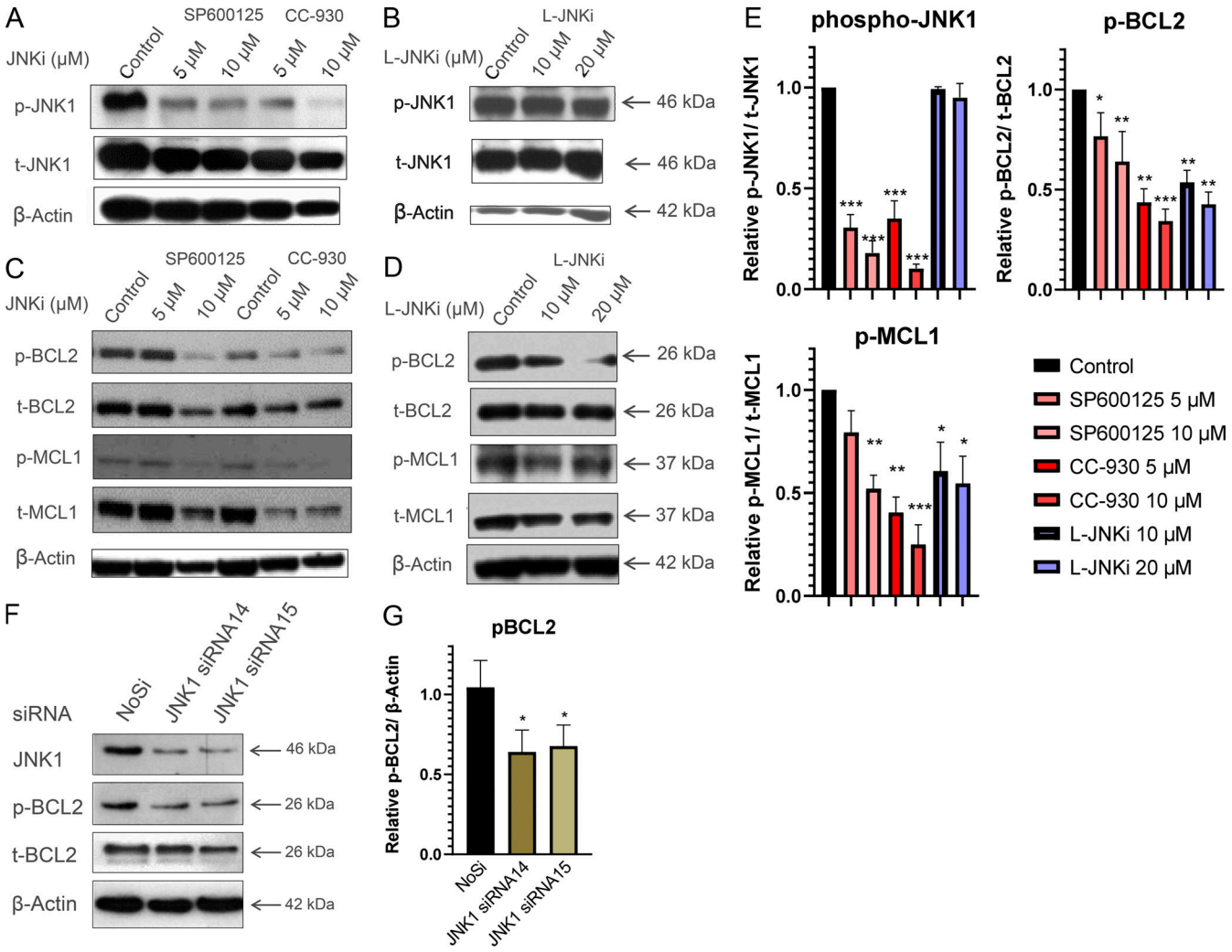

Figure 3. **JNK1 inhibition reduces the expression of the anti-apoptotic proteins BCL2 and MCL1. (A)** Protein expression of p-JNK1 and total JNK1 in primary human CLL cells after 4 h of SP600125 and CC-930 treatment (n = 3, shown CLL#8). **(B)** Protein expression of p-JNK1 and total JNK1 in primary human CLL cells after 8 h of L-JNKi treatment (CLL#34). **(C)** Protein expression of p-BCL2, total BCL2, p-MCL1, and total MCL1 in primary human CLL cells after 8 h of SP600125 and CC-930 treatment (CLL#26). **(D)** Protein expression of p-BCL2, total BCL2, p-MCL1, and total MCL1 in primary human CLL cells after 4 h of L-JNKi treatment (CLL#34). Blots are shown for one out of three CLLs per treatment. **(E)** Relative expression of pJNK1, pBCL2, and pMCL1 compared with β-actin and relative to the non-treatment control in CLL cells (n = 3) treated with the different JNK1 inhibitors (three CLLs per treatment, unpaired t test *P < 0.05; **P < 0.01, ***P < 0.001). **(F)** JNK1 expression and pBCL2/BCL2 expression in CLL cells treated with JNK1 siRNA15 and 16 or NoSi control for 24 h (CLL#34). **(G)** Relative expression of pBCL2 in CLL cells (n = 3) treated with siRNAs against JNK1 or NoSi compared with β-actin and normalized to the control group. Source data are available for this figure: SourceData F3.

and B). The relative protein expression of p-JNK1 compared with β-actin decreased by 30–50% in SYK inhibitor–treated CLL cells, 92–94% in BTK inhibitor–treated CLL cells, and 45–59% in PI3K inhibitor–treated CLL cells (Fig. 5 B). To avoid off-target effects by chemical inhibitors, we then inhibited BCR signaling by siRNA mediated knockdown of one central BCR kinase, the kinase SYK in four different CLLs. SYK knockdown in CLL cells via siRNA could be achieved (31–52% knockdown efficiency) and we observed a reduction in JNK1 phosphorylation of 42–67% (Fig. 5, C and D).

Next, we correlated the activation of the BTK kinase (intracellular phosphorylation measured by flow cytometry) with phosphorylation levels of JNK1 in untreated CLLs. The activation of BTK and JNK1 was positively correlated, implicating a higher activity of JNK1 in BCR-active CLLs (Fig. 5 E). JNK1 inhibitor-responsive samples were also responsive to SYK and BTK inhibitor treatment in a dose-dependent manner (Fig. 5 F). While JNK1 phosphorylation was directly associated with BCR signaling, this was not the case for JNK1 transcription. Neither BCR activation in normal B cells nor BCR inhibition in CLL cells directly affected JNK1 transcript levels, and only long-term BCR inhibition reduced JNK1 transcription in CLL, implicating an indirect BCR-mediated influence (Fig. S4).

JNK1 inhibition decreases leukemic burden and improves immune responses in Eμ-TCL1 mice

Next, we aimed to understand if JNK1 inhibitors are also effective in preventing CLL expansion in vivo. Therefore, we tested

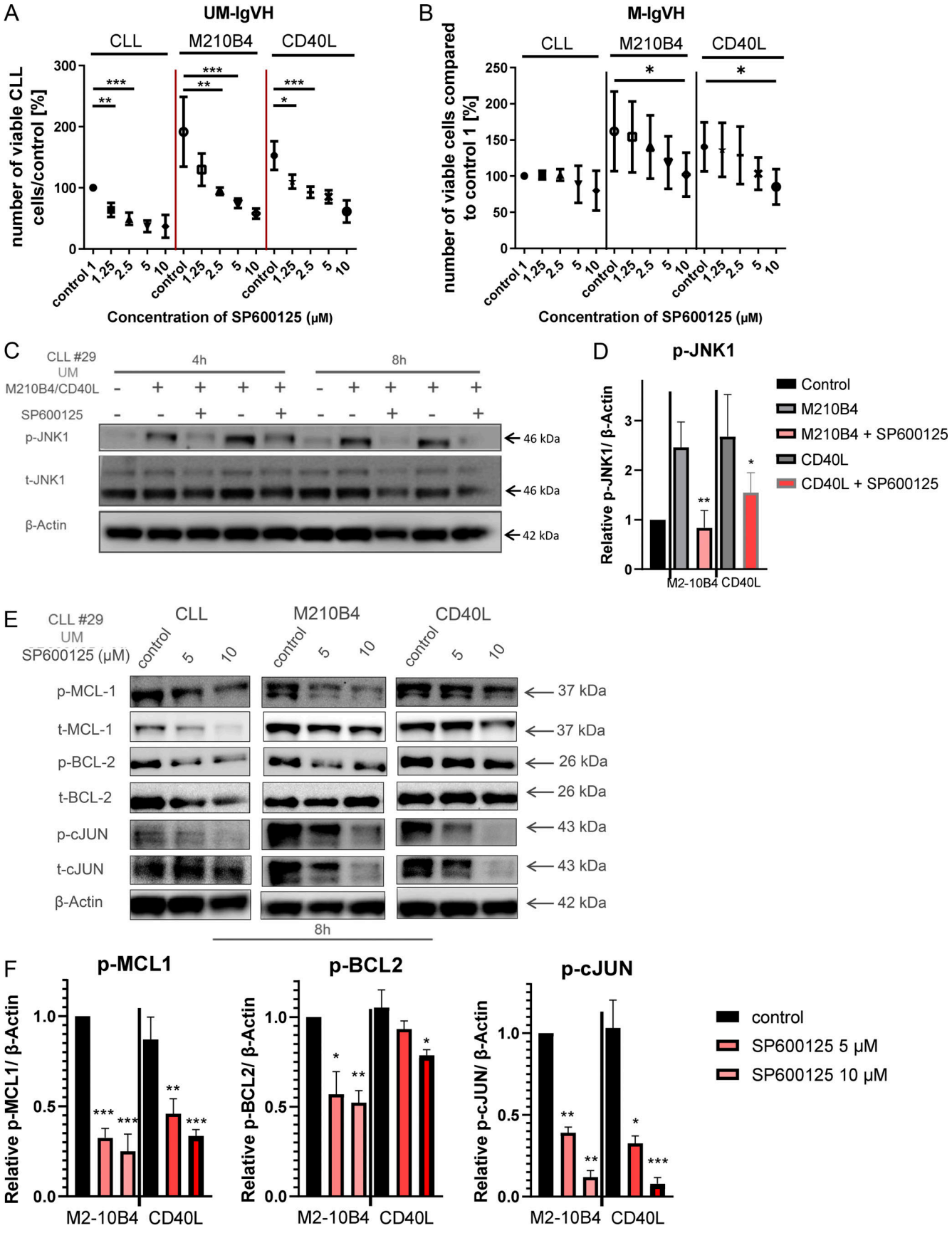

Figure 4. **JNK1 inhibitors overcome TME-induced resistance mechanisms like the upregulation of antiapoptotic proteins. (A and B)** Viability of IGHV unmutated (A, *n* = 11) or mutated (B, *n* = 12) CLL samples with or without stromal co-culture (M2-10B4 or CD40L secreting cells) after 24 h of SP600125

treatment (unpaired *t* test, *P < 0.05; **P < 0.01, ***P < 0.001). **(C)** Protein expression of p-JNK1 and total JNK1 in primary human CLL cells with or without stromal co-culture (M2-10B4 or CD40L secreting cells) and after 4 and 8 h of SP600125 treatment (CLL#29). **(D)** Relative expression of p-JNK1 in CLL samples either untreated, co-cultivated with M2-10B4 cells, or with CD40L secreting cells ± SP600125 treatment compared with β-actin and normalized to the control group (n = 4 CLLs) (unpaired *t* test, *P < 0.05). **(E)** Protein expression of p-c-JUN, c-JUN, p-BCL2, BCL2, p-MCL1, and MCL1 in primary human CLL cells with or without stromal co-culture (M2-10B4 or CD40L secreting cells) and after 8 h of SP600125 treatment (CLL#29). **(F)** Relative expression of p-MCL1, p-BCL2 and p-cJUN in CLL samples (n = 4) with or without stromal co-culture (M2-10B4 or CD40L secreting cells) and after 8 h of SP600125 treatment compared with β-actin and normalized to the control group. Statistical significance was calculated via a two-tailed unpaired *t* test (*P < 0.05; **P < 0.01, ***P < 0.001). Source data are available for this figure: SourceData F4.

the efficacy of the JNK1 inhibitor SP600125 in the Eμ-TCL1-tg mouse model, which simulates an aggressive form of human CLL. Furthermore, Eμ-TCL1 mice have an intact immune system. Mice develop a murine CLL-like disease with expansion of CD5/CD19 double positive lymphocytes in PB, BM, and spleen within 1 year after birth and evolve progressive anemia and thrombocytopenia. First, we used 20 TCL1-tg mice with increased CLL-like cells (>15,000/μl) in the PB and started individual treatments in pairs with either vehicle control or SP600125 for 3 wk and followed their individual white blood cell counts (WBC) and quantity of CLL-like cells in the PB. JNK1 inhibitor treatment reduced WBC counts and CLL cells in the PB of the individual mice, while WBC counts and CLL cells increased or stayed stable in the control group (Fig. 6, A and B). As disease onset and disease activity differ strongly between individual Eμ-TCL1-tg mice, we then aimed to use a more homogeneous system for our treatment experiments and pooled malignant CLL-like cells from spleens of three diseased mice and transplanted them into 20 irradiated C57BL/6J recipients. JNK1 inhibitor treatment or vehicle treatment (n = 10 from each group) of syngeneic transplanted TCL1 mice started after mice had developed a CLL-like disease with >40% CLL cells in the PB. Treatment continued for 3 wk, and no changes in mouse weight were seen. JNK1 inhibition strongly reduced WBC counts and CD5/CD19 double-positive CLL cells in the PB compared with controls and prevented anemia and thrombocytopenia (Fig. 6 C). Furthermore, SP600125 treatment blocked the expansion of CLL-like cells in the spleen and normalized spleen and liver weights (Fig. 6, D–F), indicating strong effects of JNK1 inhibition on CLL development in TCL1 mice.

To validate the on-target effect in vivo, we isolated residual CLL-like cells from spleens of mice treated 3 wk with vehicle or JNK1 inhibitor. In JNK1 inhibitor-treated mice, the CLL-like cells showed strong dephosphorylation of JNK1, BCL2, c-JUN, and MCL1, and also total protein levels for c-JUN and MCL1 were strongly reduced (Fig. 6, G and H). CLL cells induce an immunosuppressive environment and suppress T cell functionality. As previous studies have shown that JNK1 is involved in T cell differentiation, we also investigated the effect of JNK1 inhibition on the T cell compartment in TCL1-tg mice. While total $CD4^+$ and $CD8^+$ T-cells were not significantly affected (Fig. 6 I), we found a strong reduction in the absolute numbers of immunosuppressive regulatory T cells (Tregs) ($CD4^+CD25^+FOXP3^+$) (1.38×10^6 in vehicle-treated mice to 0.56×10^6 in JNK1 inhibitor–treated mice) (Fig. 6 J). Furthermore, JNK1 inhibition significantly enhanced the cytotoxic function of $CD4^+$ effector T cells, which are involved in the degranulation process (Fig. 6 K), thus implicating the effects of JNK1 also on T cell functions in CLL. In contrast to CLL-like cells, normal B cell numbers in spleens of healthy mice were not altered after treatment with SP600125, which indicates the selectivity of JNK1 as a target for CLL cells compared with the majority of B cells.

JNK1 inhibition blocks ibrutinib-refractory CLL in vitro and in vivo

Human CLL is more complex and more heterogeneous than TCL1 driven CLL in mice. Therefore we developed a patient-derived xenograft model for CLL, where we can engraft all subtypes of CLL, and proved its functionality for treatment studies with BCR inhibitors (Decker et al., 2019). To prove the efficacy of JNK1 inhibitors in primary CLL xenografts, we injected CLL cells from two unmutated and one mutated CLL patient into eight NOG (NOD/Shi-scid/IL-2R-gamma^{null}) mice per patient. Treatment started 1 wk after engraftment for a total of 2 wk. Spleen weight and quantity of human CLL cell numbers in the spleen and PB were assessed. Interestingly, in all three models, we found a reduction in spleen infiltration, including reduced spleen weight and reduced quantity of human CLL cells in the spleen and the PB (Fig. 7, A–C). JNK1 inhibitors were more effective in IGHV unmutated CLL samples (#27, #11), which also showed a stronger engraftment, but was also present in the IGHV mutated (#21) CLL xenograft model.

In our previous experiments, we found JNK1 to be downstream of the BCR signaling pathway. We therefore hypothesized that JNK1 inhibitors would be functional in BTK inhibitor–resistant CLLs with upstream mutations within the BCR pathway. Therefore, we treated three BTK inhibitor–resistant CLLs (two ibrutinib refractory, one tirabrutinib + SYK-inhibitor entospletinib refractory) with mutations in BTK or PLCγ2 with the JNK1 kinase inhibitor SP600125 and the substrate binding inhibitor JNKi. All BTK/SYK inhibitor-resistant CLLs responded to the JNK1 inhibitor treatment, indicating responsiveness to JNK1 inhibitors even in BTK inhibitor–resistant CLLs (Fig. 7, D and E). Next, we used CLL cells from patient #56 with BTK and SYK inhibitor resistance in our CLL xenograft model and engrafted a total of 12 NOG mice. Treatment with the JNK1 inhibitor SP600125 (100 mg/kg) was started after 1 wk of engraftment and was applied for 2 wk. JNK1 inhibitor treatment strongly reduced the amount of human $CD45^+$ cells (Fig. 7 F) and CLL cells (Fig. 7 G) in the PB and spleens of the xenografted mice (Fig. 7, G–J) and efficiently inhibited spleen and liver enlargement (Fig. 7, K and L). IHC staining for human CD79a, which marks human CLL cells in the spleens of the xenografted mice, showed a strong reduction of human CLL cells upon SP600125 treatment (Fig. 7 J). Our data indicate the activity of JNK1

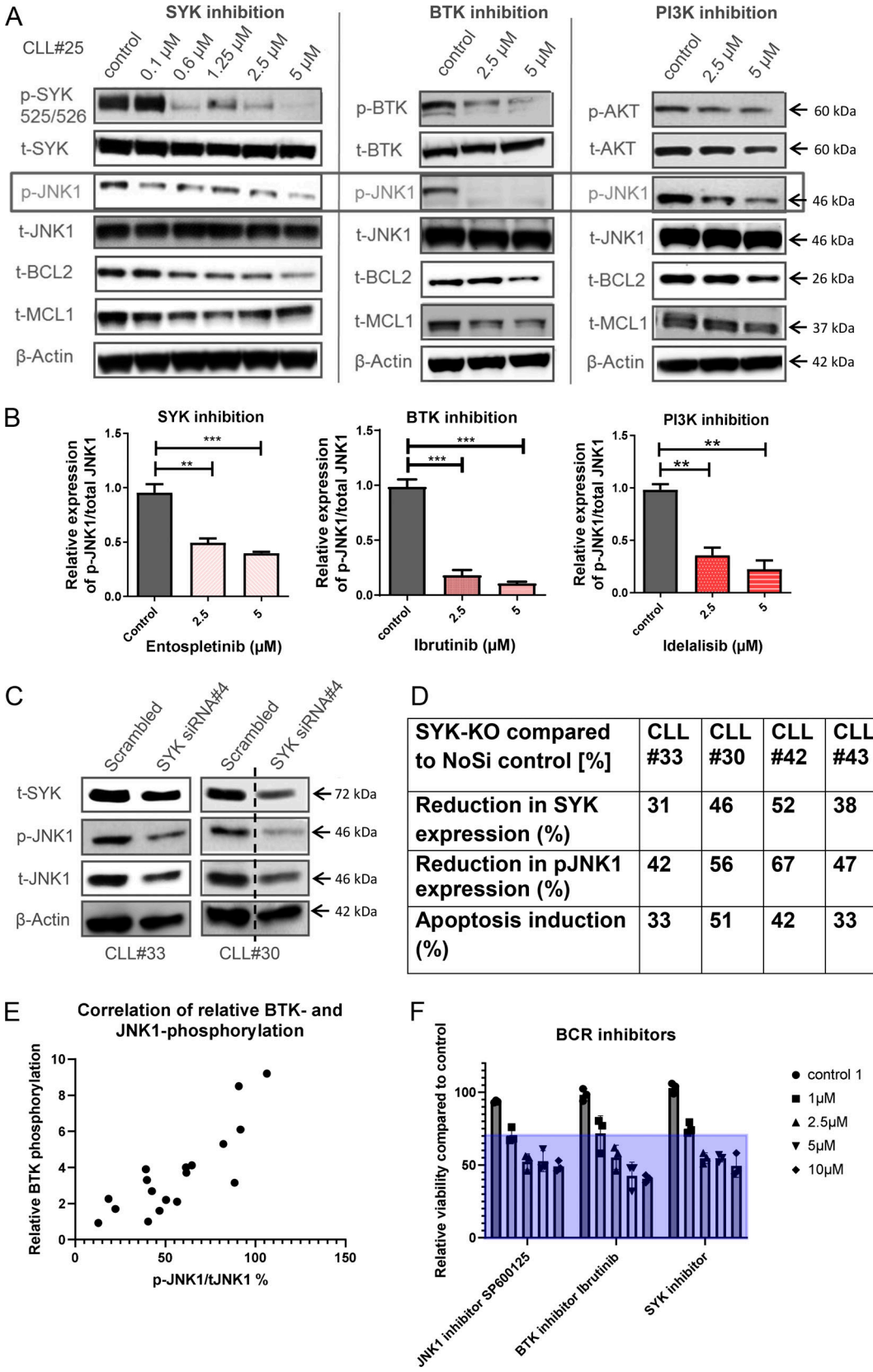

SYK-KO compared to NoSi control [%]	CLL #33	CLL #30	CLL #42	CLL #43
Reduction in SYK expression (%)	31	46	52	38
Reduction in pJNK1 expression (%)	42	56	67	47
Apoptosis induction (%)	33	51	42	33

Figure 5. **JNK1 is downstream of the proximal BCR kinases BTK, SYK, and PI3K. (A)** Protein expression of BCR signaling kinases pSYK, SYK, pBTK, BTK, and pAKT and AKT, p-JNK1, total JNK1, total BCL2, and total MCL1 in CLL cells after 8 and 24 h of treatment with the SYK inhibitor entospletinib, the BTK inhibitor ibrutinib, or the PI3K inhibitor idelalisib (CLL#25). **(B)** Relative expression of p-JNK1 compared with total JNK1 after 4 h of treatment with entospletinib, ibrutinib, and idelalisib (n = 3 CLLs) (unpaired t test, **P < 0.01, ***P < 0.001). **(C)** Protein expression of SYK, p-JNK1, and total JNK1 in primary human CLL cells

after 24 h of siRNA-mediated SYK knockdown (CLL#33 and #30). **(D)** Knockdown efficiency of SYK (24 h), relative protein expression of p-JNK1 compared with total-JNK1 (24 h), and reduction of CLL cell viability after SYK knockdown compared to control (48 h) (n = 4 different CLLs). **(E)** Relative BTK phosphorylation compared with relative JNK1 phosphorylation in CLL (n = 19) (raw data in Fig. S1, statistical analysis via Pearson correlation coefficient). **(F)** BCR inhibitors against BTK (ibrutinib) and SYK (entospletinib) were compared with the JNK1 inhibitor SP600125 in their ability to reduce viability of three CLL patient samples in vitro. Source data are available for this figure: SourceData F5.

inhibitors even in BTK/SYK inhibitor–resistant CLLs in vitro and in vivo.

Discussion

Despite remarkable treatment options and a growing number of patients in long-term remission, CLL remains a largely incurable malignancy. Current therapeutic options with BTK and BCL2 inhibitors accompanied by CD20 antibodies have high treatment potential, but relapses or drug intolerance occur and patients require alternative treatment options. In contrast to most other malignancies, the disease drivers for CLL are not oncogenic mutations or loss of tumor suppressors, but rather the chronic activation of the BCR pathway and protective signals coming from the microenvironment. Kinase targets involved in these processes are often hyperphosphorylated and overexpressed rather than mutated.

In our study, we found the serine–threonine kinase JNK1 to be widely overexpressed and additionally hyperphosphorylated in CLL (Fig. 1) compared with normal B cells and reactive lymph nodes. The other JNK kinases JNK2 and JNK3 were not increased or systematically altered in CLL, implicating a specific role for JNK1 in this disease. Interestingly, hyperphosphorylation but also the response to JNK1 inhibitors were more prominent in IGHV unmutated CLLs, the subgroup of CLL with a dismal prognosis and an increased BCR pathway activity. The same response pattern of improved response to IGHV unmutated samples has been previously shown for BTK and SYK inhibitors (Buchner et al., 2009), driving the hypothesis that JNK1 is connected with those kinases and might be involved in BCR signaling. Indeed, BTK phosphorylation levels, as a surrogate for BCR activity, are positively correlated with JNK1 phosphorylation. Furthermore, BCR pathway inhibition upstream of JNK1 by BTK, SYK, or PI3K inhibitors or SYK knockdown all reduced JNK1 phosphorylation, implicating JNK1 downstream of the other BCR kinases within the BCR signaling pathway (Fig. 5). Previous publications in anti-IgM activated normal B cells also located JNK1 downstream of SYK, BTK, and PLCγ2, and identified BCR-mediated calcium signaling as well as PKC phosphorylation to be required for JNK1 phosphorylation (Inabe et al., 2002; Jiang et al., 1998). Interestingly, anti-IgM stimulation of CLL cells did not further increase JNK1 phosphorylation in the majority of samples, which implicate that the hyperactive BCR in CLLs already extended the BCR-induced JNK1 phosphorylation level to a maximum (Petlickovski et al., 2005).

While JNK1 phosphorylation is directly connected to the BCR, this is less clear for JNK1 transcription. Baseline transcript levels for JNK1 are increased in CLL compared with normal B cells (Fig. 1, A and B). While short-term BCR inhibition has no influence on JNK1 transcription, long-term BCR inhibition reduces JNK1 transcript levels, which implicates that an indirect effector regulated by the tonic active BCR receptor regulates JNK1 transcript levels in CLL.

The tumor microenvironment (TME) is another important factor supporting CLL survival and proliferation and consists of nurse-like cells, mesenchymal stem cells (MSCs), fibroblasts, T cells, and other local cells within lymph nodes and BM. The TME directly induces activation of BCR signaling, resulting in the proliferation of CLL cells in the lymph node, whereas circulating CLL cells isolated from blood tend to be resting and in a quiescent state (Herishanu et al., 2011). CLL cells and TME interact via direct cell–cell contact or via secreted cytokines and growth factors. Major pathways directing the interaction of CLL cells with nurse-like cells and MSCs are the CXCL12/CXCR4 signaling axis, and T cells interact via the CD40/CD40L axis. BTK and SYK are downstream of both pathways and BTK inhibition causes mobilization of CLL cells out of lymph nodes and at a later time point also out of the BM causing a so-called leukocyte flair in the initial therapeutic phase. Interestingly, the co-culture of CLL cells with CXCL12-producing M2-10B4 cells or CD40-ligand–producing cells induced a strong JNK1 phosphorylation in CLL cells and a simultaneous upregulation and phosphorylation of antiapoptotic genes like BCL2 and MCL1. JNK1 inhibition in this co-culture context normalized BCL2 and MCL1 phosphorylation, indicating that it is similarly effective as ibrutinib in blocking stroma protective effects. In IGHV-mutated CLLs, the inhibition of TME protective effects might be even more important than the inhibition of BCR signaling (Fig. 4 B and Fig. 7 A). In contrast to ibrutinib treatment, we did not observe a leukocyte flair in our different in vivo models (no enhanced CLL cells in PB after treatment initiation), which might be due to the short treatment period or caused by the strong direct proapoptotic effect of the JNK1 inhibitors.

Previous publications indicated that JNK1 phosphorylation might even have a proapoptotic function in CLL in the context of arsenic trioxide or oxazepine-based anticancer agents (Redondo-Muñoz et al., 2010; Vanni et al., 2021). Our findings that hyperphosphorylation of JNK1 in CLL compared with normal B cells is common, that the protective microenvironment further induces hyperphosphorylation of JNK1, as well as the clear effects of JNK1 inhibitors or JNK1 kd on apoptosis induction in the majority of CLLs clearly support an opposite role as an important antiapoptotic kinase. As shown in previous publications, JNK1 mediates the phosphorylation of Bcl2 at residues T69, T70, and T87, which mediate the interaction of Bcl2 with Beclin1 and regulates prosurvival processes like autophagy (Wei et al., 2008a). In addition, long-term activation of JNK1 and increasing Bcl2 phosphorylation induce dissociation of Bcl2 and Bax, which causes cleavage of Caspase 3 and induces classical apoptosis (Wei et al., 2008b). The balance of Bcl2

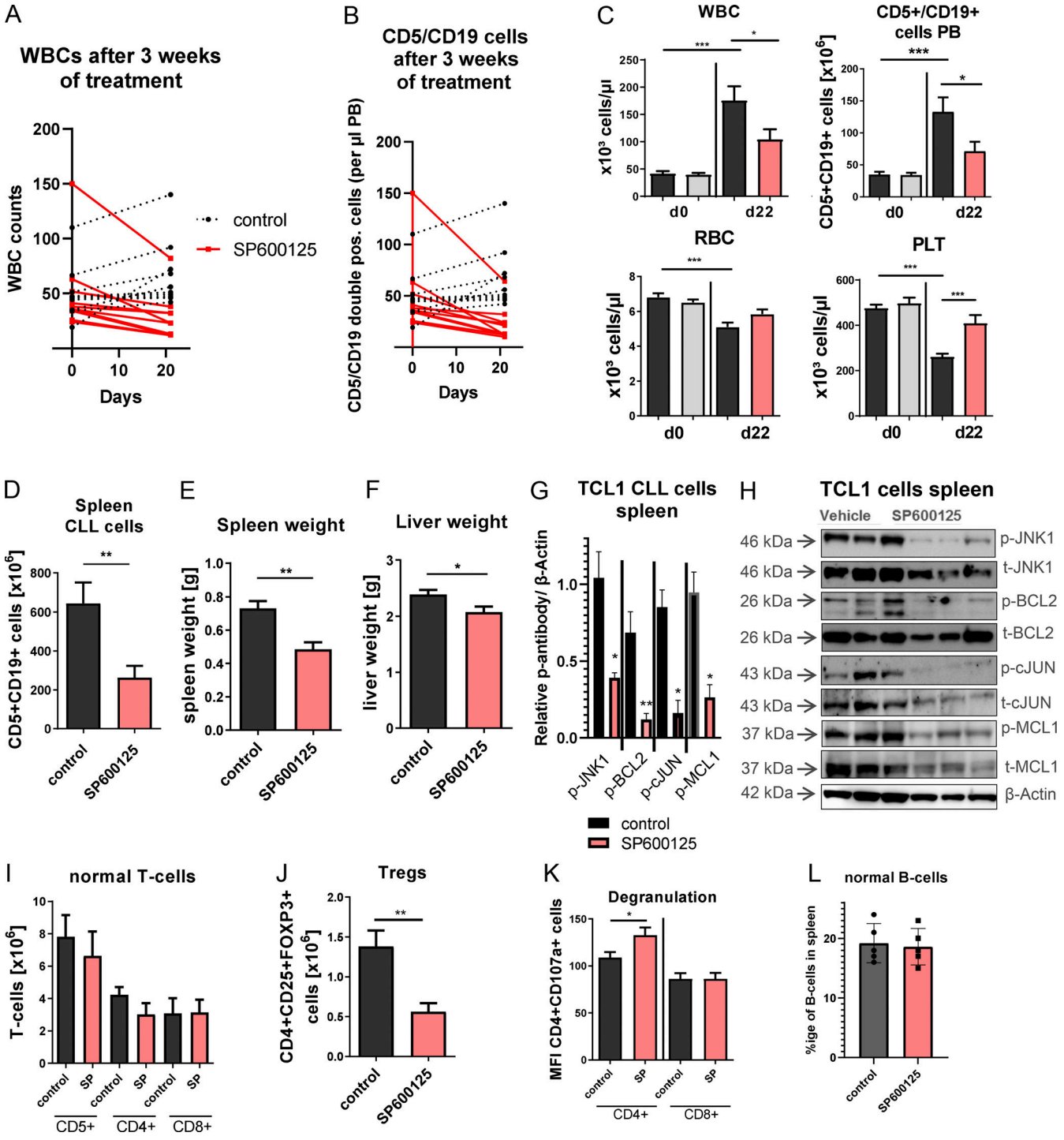

Figure 6. **JNK1 inhibition decreases leukemic burden and modulates immune responses in Eμ-TCL1 mice. (A and B)** WBC counts or (B) quantity of CLL-like CD19⁺/CD5⁺ cells of TCL1-tg mice treated with vehicle control or the JNK1 inhibitors SP600125 for 3 wk shown before and after treatment (10 mice in each treatment group). **(C)** 20 C57BL6 mice were sublethally irradiated and transplanted with splenocytes of three diseases TCL1-tg mice and used for treatment experiments after disease development. Graphs show WBC, RBC, platelet (PLT) counts and quantity of CD19⁺CD5⁺ CLL-like cells in the PB after 3 wk of SP600125 or vehicle treatment (n = 10 per group, unpaired t test, *P < 0.05; ***P < 0.001). **(D–F)** Total number of CD5⁺CD19⁺ cells per spleen (D), spleen weight (E), and liver weight (F) in TCL1-Tx mice after 3 wk of SP600125 treatment (unpaired t test, *P < 0.05; **P < 0.01). **(G)** Relative protein levels of p-JNK1, p-BCL2, p-cJUN, and pMCL1 in sorted CD5⁺/CD19⁺ cells from spleens of TCL1-Tx mice after 21 d of SP600125 treatment (unpaired t test, *P < 0.05; **P < 0.01). **(H)** Protein levels of p-JNK1, total JNK1, p-BCL2, total BCL2, p-c-Jun, total c-Jun, p-MCL1 and total MCL1 in sorted CD5⁺/CD19⁺ cells of TCL1-Tx mice after 21 d of SP600125 treatment. **(I)** Total number of CD5⁺, CD4⁺, and CD8⁺ T cells in spleens of SP600125-treated TCL1-Tx mice. **(J)** Absolute number of Tregs in the spleens of TCL1-Tx mice after 3 wk of SP600125 treatment (n = 10 per group, unpaired t test, **P < 0.01). **(K)** CD107a expression as marker for degranulation of CD4⁺ and CD8⁺ T cells in the spleens of TCL1-Tx mice after 21 d of SP600125 treatment (n = 10 mice per group). **(L)** Graph shows the percentage of B cells (CD19⁺, B220⁺) in spleens of C57/Bl6 mice (n = 5 per group) treated with vehicle control or the JNK1 inhibitor SP600125 for 3 wk. Statistical significance was calculated via a two-tailed unpaired t test (*P < 0.05; **P < 0.01, ***P < 0.001). Source data are available for this figure: SourceData F6.

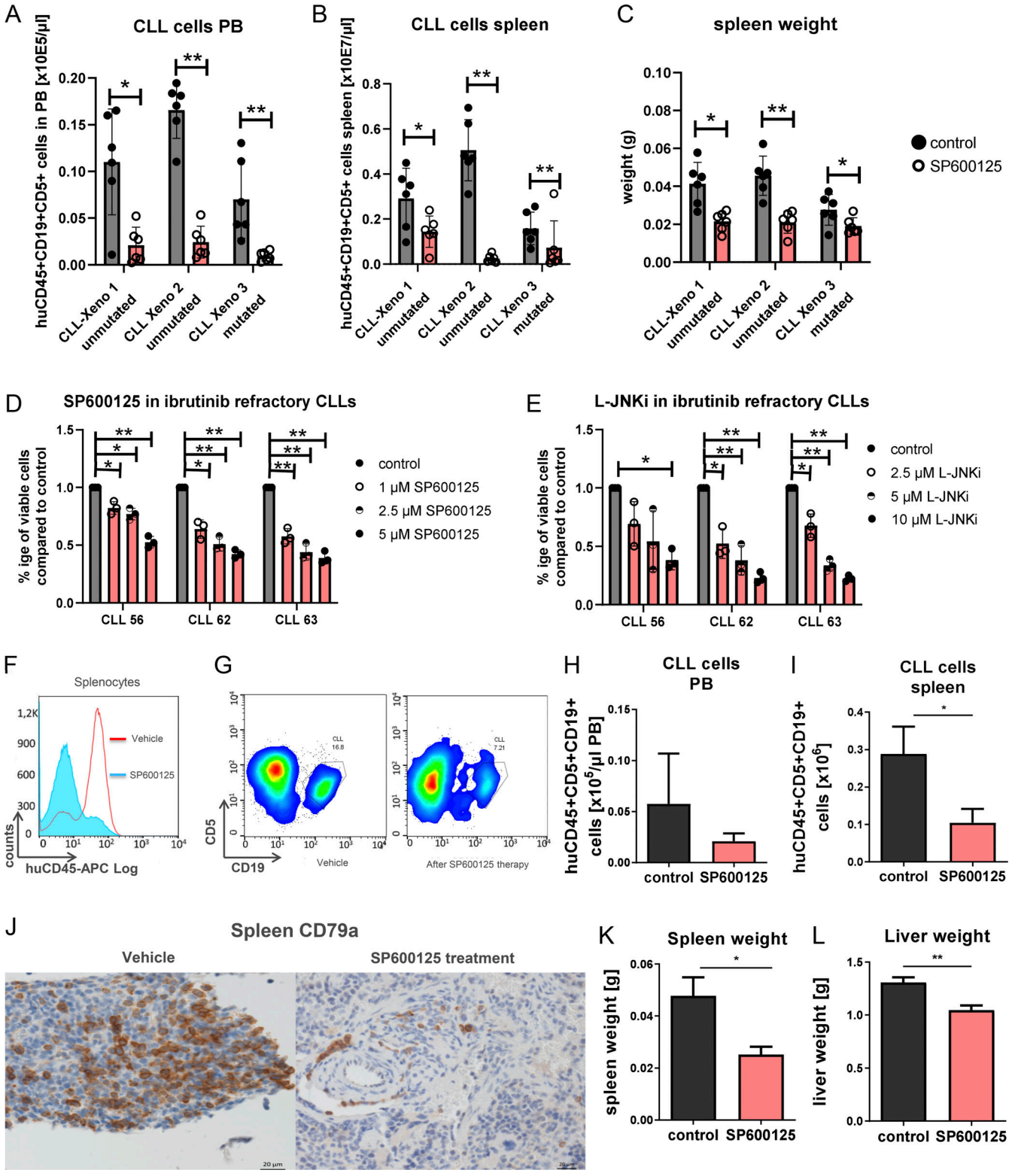

Figure 7. **JNK1 inhibition reduces CLL cell expansion in patient-derived xenograft (PDX) mouse models for normal and ibrutinib refractory CLL. (A)** HuCLL cells ($CD45^+CD5^+CD19^+$) in the PB of mice (n = 6 per CLL) xenografted with three different CLLs and treated with vehicle control or SP600125 for 2 wk (pts #34, 60, and 8, unpaired t test, *P < 0.05; **P < 0.01). **(B and C)** HuCLL cells in the spleen (B) and (C) spleen weight in the same experiment after 2 wk of JNK1 inhibitor treatment of xenografted mice (unpaired t test, *P < 0.05; **P < 0.01). **(D and E)** Treatment of three BTK-inhibitor refractory CLLs with different concentrations of JNK1 inhibitors (CLL#56, #62, #63, unpaired t test, *P < 0.05; **P < 0.01). **(F)** Engraftment of a BTK- + SYK-inhibitor refractory CLL (#56): Human $CD45^+$ cell engraftment in the spleen of an SP600125-treated mouse (blue) compared with a vehicle-treated mouse (red). **(G)** Flow cytometry plots showing the percentage of CLL cells in the spleen after 14 d of SP600125 treatment (vehicle:16.8%; SP600125: 7.21%). **(H and I)** Absolute number of CLL cells in the blood (H) and (I) in the spleen of xenografted NOG mice after 14 days of the vehicle or SP600125 treatment (n = 6 per group, unpaired t test,

*P < 0.05; **P < 0.01). **(J)** IHC staining for human CD79a in the spleens of CLL xenograft mice after 2 wk of SP600125 treatment (scale bar: 20 µm). **(K and L)** Spleen and liver weights of CLL-transplanted NOG mice after 14 d of SP600125 treatment (n = 6 per group). Statistical significance was calculated via two-tailed unpaired t test (*P < 0.05; **P < 0.01).

phosphorylation regarding signal strength (phosphorylation level) and latency of phosphorylation is highly delicate and long-term phosphorylation driven by JNK1 hyperphosphorylation might strongly alter its normal function balancing autophagy and apoptosis in CLL cells. Additional publications reported that the protein stability of Bcl2 is also regulated via JNK1 phosphorylation, and that treatment of breast cancer cells with JNK1 inhibitors causes the destabilization of prosurvival complexes driving early microtubule inactivation to induce apoptosis (Kelkel et al., 2012).

In addition to Bcl2, JNK1 also phosphorylates several residues on Mcl1, and short-term activation of JNK1 causes Mcl1 phosphorylation, polyubiquitinylation, and degradation. On the other hand, tonic T cell receptor signaling as being similar to tonic BCR signaling in CLL induces the TAK1–JNK pathway causing long-term Mcl1 phosphorylation and induces Mcl1 stabilization. In this situation, JNK1 dephosphorylation causes destabilization of Mcl1 and protein degradation, driving apoptosis (Hirata et al., 2013).

CLL patients suffer from severe immunosuppression with reduced activity of B and T cells against infectious diseases and have a higher rate of secondary malignancies. This immunosuppressive environment includes reduced immunoglobulin levels, reduced B and T cell activity, and an increased amount of FOXP3$^+$ Tregs, which are known to broadly suppress the immune system. Current CLL therapies even further reduce the ability of the immune system to react to infectious complications. CD20 antibodies like rituximab/obinutuzumab diminish also normal B cells and further reduce immunoglobulin levels. The BCL2 inhibitor venetoclax reduces all cell types including myeloid and lymphoid cells and causes severe immunosuppression. At least within the Eµ-TCL1 mouse model, we found that JNK1 inhibitors might be able to improve T cell functionality and enhance the cytotoxic effect of CD4$^+$ T cells while reducing the number of immunosuppressive Tregs. Furthermore, thrombocytes and RBCs even increased in JNK1 inhibitor-treated TCL1 mice, but further studies in humans are needed to verify those results in a broader context.

BTK-targeting agents like ibrutinib, acalabrutinib, or zanubrutinib or SYK inhibitors like entospletinib are the most common BCR inhibitors used in the clinic (Burger et al., 2015). Longterm outcomes are mainly available for ibrutinib, and here the presence of primary or acquired resistance is common (20–30%) and often leads to dismal clinical outcomes and even to a more aggressive disease after cessation of the inhibitor (George et al., 2020; Valla et al., 2018). Several studies have identified resistance mechanisms to ibrutinib in CLL (Furman et al., 2014; Woyach et al., 2014). About 80% of the patients develop acquired resistance due to clonal expansion of CLL cells carrying mutations within BTK (BTK C481S) or activating/gain of function mutations in PLCγ2 (Furman et al., 2014; Woyach et al., 2014; Lampson and Brown, 2018; Ahn et al., 2017). Other genetic resistance mechanisms causing reduced drug sensitivity include mutations in p53, CARD11, SF3B1, del17p, or del 8p (Amin et al., 2017; Kanagal-Shamanna et al., 2019; Burger et al., 2016) or changes in the TME, and efforts need to be made to overcome these processes. Interestingly JNK1 inhibition was effective in vitro and in vivo in inducing apoptosis in three CLL patient samples with acquired ibrutinib (2×) or tirabrutinib + SYK inhibitor resistance, which indicates that JNK1 inhibitors can overcome BTK inhibitor resistance. The JNK1 inhibitor CC-90001, which is based on the inhibitor CC-930 is already in clinical development and has passed a phase I/II trial in patients with pulmonary fibrosis (Nagy et al., 2021; Popmihajlov et al., 2022; Ye et al., 2022). Similar to what is seen for all BCR inhibitors, side effects included increased infection rates like respiratory tract infections (21%), which might be due to an altered BCR activation of normal B cells. Other cell types like erythrocytes, thrombocytes, granulocytes, or T cells were not affected within the trials, and in our mouse experiments, erythrocytes and thrombocytes even recovered during JNK1 inhibitor treatment of TCL1 mice (Fig. 6). Based on our results, we aim to initiate a clinical trial with CC-90001 in CLL patients, which are refractory to BTK or SYK inhibitors, and will accompany treatments with a special few on normal B cell function (IgG levels, B cell functionality) and preventive measures regarding infections.

Taken together, our experiments identified JNK1 as a promising novel drug target in CLL downstream of the BCR, which can overcome BTK-inhibitor resistance, block microenvironmental protective effects, and additionally improve immune functions in CLL patients.

Materials and methods

CLL patient samples

This study was approved by the Institutional Review Board of the University Medical Center Freiburg. PB samples were obtained with informed consent in accordance with the declaration of Helsinki from CLL patients who were either untreated or off therapy for at least 6 mo. CLL samples were characterized for IGHV mutational status, disease stage according to the Binet and Rai criteria, and history of treatment. Furthermore, genetic aberrations were analyzed by chromosomal analysis and FISH analysis, and copy number changes were verified by SNP arrays (Pfeifer et al., 2007) (patient characteristics are shown in Table S1). CLL-PB mononuclear cells (CLL-PBMCs) were separated by Ficoll gradient centrifugation and either used fresh or were cryopreserved in fetal calf serum (FCS) with 10% dimethyl sulfoxide (DMSO) until use. Cells were maintained in a DMEM medium with 10% FCS and 1% penicillin–streptomycin. CLL-PBMCs for RNA isolation or western blot contained >90% CD19$^+$/CD5$^+$ CLL cells. Cells were lysed in RLT buffer for RNA extraction or deep-frozen for protein extraction and subsequent immunoblotting.

Cell lines

The murine BM stromal cell line M2-10B4 (RRID:CVCL_5794, ATCC; CRL-1972) and the human CD40-ligand producing cell line 3T3-msCD40L (RRID:CVCL_1H10) (Liebig et al., 2009; Raptis and Bolen, 1989) were both cultured in DMEM supplemented with 10% FCS and 1% penicillin–streptomycin.

Small molecules

The JNK1 inhibitors SP600125 (Selleckchem) and CC-930 (MedChem Express) are ATP-competitive small-molecule inhibitors. The JNK1 inhibitor L-JNKi 1 (MedChem Express) is a substrate-binding inhibitor. The BTK inhibitor ibrutinib, the PI3K inhibitor idelalisib (p110δ), and the SYK inhibitor entospletinib (all from Selleckchem) are kinase inhibitors targeting upstream BCR signaling.

Apoptosis assay

CLL-PBMCs were plated onto 96-well plates at a concentration of 1×10^5 cells/well with or without support of the murine stromal cell line M2-10B4 (RRID:CVCL_5794, CRL-1972; ATCC) or NIH3T3/tCD40L cells (RRID:CVCL_1H10). In the case of stromal co-culture, 5×10^3 stromal cells/well were plated in 100 µl of medium containing DMEM with 10% FCS and 1% penicillin–streptomycin. After 24 h, CLL-PBMCs were added and treated with JNK1 inhibitors (SP600125, CC-930, and L-JNKi), ibrutinib, idelalisib, or entospletinib at the indicated concentrations. After 24 and 48 h of incubation at 37°C in 5% CO_2, cells were stained with CD5-V450 (Clone L17F12, Cat#644487; BD Bioscience) and CD19-APC antibody (SJ25C1; BD Bioscience; RRID:AB_1645728), followed by AnnexinV/7-AAD staining (BD) according to the manufacturer's instructions. Cells were analyzed using the CyanADP flow cytometer (Beckman Coulter). Flow cytometry data were analyzed using the FlowJo 7.6 software (Tree Star, FlowJo, RRID:SCR_008520) (Van Gassen et al., 2015).

siRNA-mediated knockdown

Freshly isolated PBMCs (1×10^7) were suspended in nucleofection solution (Nucleofector kit V; Lonza), and siRNAs (JNK1: SI02758651, SI02758644, SI02758637, and SI02757209; SYK: SI00048741; Qiagen) were added at a concentration of 20 µmol/liter. Transfection was performed using the U-013 program of Amaxa Biosystems Nucleofector II (Amaxa Biosystems). Then, cells were suspended in DMEM with 10% FBS and cultured for 36 h. Then half of the cells were stained with CD19-APC, CD5-V450, AnnexinV-PE/7-AAD (BD Biosciences), and viability was analyzed by flow cytometry as described above. Cell lysis was performed with the other half of the transfected CLL cells and knockdown efficiency for JNK1 as well as p-BCL2 or total BCL2 expression was calculated by ImageJ software (ImageJ, RRID:SCR_003070) (Van Gassen et al., 2015) relative to β-actin and compared with non-silencing control (D-001206-14-05; Dharmacon).

Immunoblotting

Protein expression of JNK1 (2C6) (Cat#3708; Cell Signaling Technology, RRID:AB_1904132), p-JNK1 (Cat#8206; Cell Signaling Technology, RRID:AB_1658223), c-JUN (Cat#sc-74543; Santa Cruz Biotechnology, RRID:AB_1121646), p-c-JUN (Cat#sc-822; Santa Cruz Biotechnology, RRID:AB_627262), BCL-2 (Cat#sc-7382; Santa Cruz Biotechnology, RRID:AB_626736), phospho-BCL-2 (Thr56) (Cat#2875; Cell Signaling Technology, RRID:AB_2243462), MCL-1 (D35A5) (Cat#5453; Cell Signaling Technology, RRID:AB_10694494), phospho-MCL-1 (Thr163) (D5M9D) (Cat#14765; Cell Signaling Technology, RRID:AB_2716686), SYK (D1I5Q) (Cat#12358; Cell Signaling Technology, RRID:AB_2687923), phospho-SYK (Tyr352) (Cat#2701; Cell Signaling Technology, RRID:AB_331600), BTK (D3H5) (Cat#8547; Cell Signaling Technology, RRID:AB_10950506), and phospho-BTK (Tyr223) (Cat#5082; Cell Signaling Technology, RRID:AB_10561017) was detected using standardized protocols (antibody list in Table S3). CLL cell lysates were prepared after exposure to JNK1 inhibitors: SP600125, CC-930, and L-JNKi; SYK inhibitor: entospletinib; BTK inhibitor: ibrutinib or PI3K inhibitor: idelalisib for 4, 8, or 24 h. Western Blots were analyzed using the ImageJ software (RRID:SCR_003070; ImageJ) (Schneider et al., 2012).

TaqMan real-time PCR

Total cellular RNA was extracted from primary human CLL cells using a Qiagen RNAeasy Mini kit. cDNA was synthesized by using oligo dT primers, Superscript II reverse transcriptase (Life technologies), and deoxynucleotides (Fermentas) according to the manufacturer's instructions. Human primers (JNK1: Hs01548508_m1, GAPDH:Hs02758991_g1) for TaqMan PCR were purchased from ThermoFisher. Results were quantified by $\Delta\Delta$-C_t method based on the relative expression of the target gene versus the reference gene (GAPDH) and normalized to the median of control samples.

In vivo studies in CLL-xenografted NOG mice

All animal experiments were approved by the institutional review board of the University Freiburg according to the declaration of animal welfare. NOG mice (NOD.Cg-Prkdc^{scid} IL2rg^{tm1Sug}/JicTac; Taconic) female mice (n = 12) were transplanted at 9–11 wk. Therefore, PBMCs of primary CLL samples were isolated within 3 h of venipuncture by Ficoll density centrifugation. The interlayer was collected, washed twice, counted, and resuspended in HBSS. A total of 7–10 × 10^8 CLL-PBMCs were directly transplanted in 0.4 ml of HBSS using both retrobulbar and intraperitoneal application. SP600125 treatment started 1 wk after transplantation and lasted 2 wk. Therefore, mice injected with CLL cells from the different patients were divided into two similar subgroups (vehicle control and inhibitor) according to the amount of CLL cells in blood, blood cell counts, and weights. SP600125 (100 mg/kg body weight [BW]) was freshly solved using an ultrasonic bath and treatment was applied according to weight using oral gavage. Disease development was monitored by daily weight measurements and biweekly blood withdrawal. After 2 wk of treatment, mice were sacrificed and spleen and BM cells were harvested and filtered. Erythrocyte lysis was followed by quantification of total cell counts and FACS staining for human CD5, CD19, and CD45 (all BD). Cells were analyzed with the CyanADP flow cytometer (Beckman Coulter) and flow cytometric data were analyzed with the FlowJo 7.6 software (FlowJo, RRID:SCR_008520) (Van Gassen et al., 2015).

In vivo studies in TCL1-tg mice

For the first treatment experiments (Fig. 7, A–C), Eμ-TCL1-tg mice were selected with at least 15 Tsd/μl CD19/CD5 double-positive CLL-like cells in the PB. Mice were matched into pairs according to their WBC count, quantity of CLL cells, and body weight and treated with SP600125 (100 mg/kg BW) daily by oral gavage for 3 wk. For the second treatment experiment (starting Fig. 7 D), splenocytes from one diseased Eμ-TCL1-tg mouse were stained with anti-mouse CD5-PE (Cat# 100607; BioLegend, RRID: AB_312737) and CD19-APC antibody (Cat# 152410; BioLegend, RRID:AB_2629838), analyzed by flow cytometry, counted, and resuspended in HBSS. C57BL/6-recipient mice (RRID:IMSR_JAX: 000664; Jackson Laboratory) (n = 20 females) were sublethally irradiated with 2 × 3.5 Gy before receiving a total of 30.0 × 10^6 $CD5^+/CD19^+$ splenocytes by retrobulbar injection. Disease development was monitored by weekly weight measurements, biweekly WBC counts, and PB-staining for murine $CD5^+/CD19^+$ double-positive cells, and mice were grouped into two equal cohorts. SP600125 or vehicle treatment for 3 wk started after mice had >30% $CD5^+/CD19^+$ cells in the PB. After 3 wk of treatment, mice were sacrificed, and spleen and BM cells were harvested and filtered. Erythrocyte lysis was followed by analyzing total cell counts and FACS staining for murine CD5 and CD19. Cells were analyzed with the CyanADP flow cytometer (Beckman Coulter), and Flow cytometric data were analyzed using FlowJo (RRID:SCR_008520; FlowJo) (Van Gassen et al., 2015).

IHC

Spleens were fixed in 4% buffered formalin. After paraffin-embedding, sections were deparaffinized in xylene and graded alcohols as described before (Decker et al., 2019). H&E and chloracetate esterase (NACE) staining followed standard protocols. After specific antigen retrieval in "low pH target retrieval solution" (Dako) for 30 min, IHC staining was performed using antibodies against human CD79a (M7050; Dako). The EnVision FLEX System (Dako) was used for signal visualization. Sections were counterstained with hematoxylin (Dako) and mounted. IHC for JNK1 (PA5-141009; Invitrogen) and p-JNK1 (Thr183; Invitrogen) was performed according to the suppliers' instructions. The Bond Polymer Refine Detection Kit (DS9800; Leica) was employed for visualization on a fully automated IHC stainer (Leica Bond). For expression analysis of JNK1 and pJNK1 H, score was employed as described previously (Seliger et al., 2022).

Statistical analysis

Data are represented as the mean ± standard error of the mean (SEM). Comparisons between parameters were performed using a two-tailed, unpaired/paired Student's t test, or the Mann–Whitney test. For all analyses, $P < 0.05$ was considered statistically significant.

Contact for reagents and resource sharing

Further information and requests for resources and reagents should be directed to and will be fulfilled by the corresponding author Christine Dierks (christine.dierks@uk-halle.de).

Online supplemental material

Fig. S1 shows the relative viability of B cells extracted from the PB of healthy donors and treated with different concentrations of JNK1 inhibitors or controls. Fig. S2 shows the distribution of response groups of CLL cells treated with the three different JNK1 inhibitors SP600125 CC-930 or the peptide inhibitor L-JNKi. Fig. S3 shows treatment of stroma cells with JNIK1 inhibitors. Fig. S4 shows JNK1 mRNA expression after ibrutinib treatment. Supplementary information includes a list of CLL patient samples including the response of individual patients to different treatments (Table S1), individual JNK1 protein and RNA expression (Table S2), and antibody list (Table S3).

Data availability

Data are available from the corresponding author upon request via e-mail christine.dierks@uk-halle.de.

Acknowledgments

The authors thank the lymphoma ambulance (Anita Bürk and Gabriele Büsch) and the core facility, especially Marie Follo for support. Furthermore, we thank Julia Huber from the Tumorbank Comprehensive Cancer Center Freiburg, Medical Center-University of Freiburg, Faculty of Medicine, University of Freiburg, Freiburg, Germany for performing the IHC stainings.

This work was supported by the Deutsche Krebshilfe via grants 111025 and 70112614. The work was further supported by the Deutsche Forschungsgemeinschaft (DFG) through the Emmy-Noether program from C. Dierks (DI 1664/1-1), through DFG grants from FOR 2033 DI 1664/2-2 and FOR DI 1664/3-1, and FOR5659 517204983 to C. Dierks. The work was further supported by the José-Carreras grants DJCLS F15/3 for S. Decker and DJCLS04F/2016 for C. Klein.

Author contributions: S.K. Saleem: Conceptualization, Data curation, Formal analysis, Investigation, Methodology, Project administration, Validation, Visualization, Writing - original draft, Writing - review & editing, S. Decker: Conceptualization, Data curation, Formal analysis, Investigation, Methodology, Project administration, Supervision, Writing - original draft, Writing - review & editing, S. Kissel: Investigation, M. Bauer: Data curation, Investigation, Writing - review & editing, D. Chernyakov: Formal analysis, Writing - review & editing, D. Bräuer-Hartmann: Investigation, Visualization, Writing - review & editing, K. Aumann: Methodology, Validation, Writing - review & editing, C. Wickenhauser: Conceptualization, Visualization, Writing - review & editing, M. Herling: Resources, Validation, O. Skorobohatko: Investigation, Writing - review & editing, N. Mathew: Methodology, C. Schmidt: Conceptualization, C. Klein: Formal analysis, Investigation, Methodology, Software, Supervision, Validation, M. Follo: Investigation, Methodology, Resources, C. Dierks: Conceptualization, Formal analysis, Funding acquisition, Investigation, Project administration, Resources, Supervision, Visualization, Writing - original draft, Writing - review & editing.

Disclosures: The authors declare no competing interests exist.

Submitted: 21 April 2023
Revised: 21 March 2024
Accepted: 8 July 2024

References

Agathangelidis, A., N. Darzentas, A. Hadzidimitriou, X. Brochet, F. Murray, X.J. Yan, Z. Davis, E.J. van Gastel-Mol, C. Tresoldi, C.C. Chu, et al. 2012. Stereotyped B-cell receptors in one-third of chronic lymphocytic leukemia: A molecular classification with implications for targeted therapies. *Blood*. 119:4467–4475. https://doi.org/10.1182/blood-2011-11-393694

Ahn, I.E., C. Underbayev, A. Albitar, S.E. Herman, X. Tian, I. Maric, D.C. Arthur, L. Wake, S. Pittaluga, C.M. Yuan, et al. 2017. Clonal evolution leading to ibrutinib resistance in chronic lymphocytic leukemia. *Blood*. 129:1469–1479. https://doi.org/10.1182/blood-2016-06-719294

Alexaki, V.I., D. Javelaud, and A. Mauviel. 2008. JNK supports survival in melanoma cells by controlling cell cycle arrest and apoptosis. *Pigment Cell Melanoma Res.* 21:429–438. https://doi.org/10.1111/j.1755-148X.2008.00466.x

Amin, N.A., S. Balasubramanian, K. Saiya-Cork, K. Shedden, N. Hu, and S.N. Malek. 2017. Cell-intrinsic determinants of ibrutinib-induced apoptosis in chronic lymphocytic leukemia. *Clin. Cancer Res.* 23:1049–1059. https://doi.org/10.1158/1078-0432.CCR-15-2921

Binder, M., B. Léchenne, R. Ummanni, C. Scharf, S. Balabanov, M. Trusch, H. Schlüter, I. Braren, E. Spillner, and M. Trepel. 2010. Stereotypical chronic lymphocytic leukemia B-cell receptors recognize survival promoting antigens on stromal cells. *PLoS One*. 5:e15992. https://doi.org/10.1371/journal.pone.0015992

Bogoyevitch, M.A., and B. Kobe. 2006. Uses for JNK: The many and varied substrates of the c-jun N-terminal kinases. *Microbiol. Mol. Biol. Rev.* 70:1061–1095. https://doi.org/10.1128/MMBR.00025-06

Buchner, M., S. Fuchs, G. Prinz, D. Pfeifer, K. Bartholomé, M. Burger, N. Chevalier, L. Vallat, J. Timmer, J.G. Gribben, et al. 2009. Spleen tyrosine kinase is overexpressed and represents a potential therapeutic target in chronic lymphocytic leukemia. *Cancer Res.* 69:5424–5432. https://doi.org/10.1158/0008-5472.CAN-08-4252

Burger, J.A., N. Tsukada, M. Burger, N.J. Zvaifler, M. Dell'Aquila, and T.J. Kipps. 2000. Blood-derived nurse-like cells protect chronic lymphocytic leukemia B cells from spontaneous apoptosis through stromal cell-derived factor-1. *Blood*. 96:2655–2663. https://doi.org/10.1182/blood.V96.8.2655

Burger, J.A., and N. Chiorazzi. 2013. B cell receptor signaling in chronic lymphocytic leukemia. *Trends Immunol.* 34:592–601. https://doi.org/10.1016/j.it.2013.07.002

Burger, J.A., A. Tedeschi, P.M. Barr, T. Robak, C. Owen, P. Ghia, O. Bairey, P. Hillmen, N.L. Bartlett, J. Li, et al. 2015. Ibrutinib as initial therapy for patients with chronic lymphocytic leukemia. *N. Engl. J. Med.* 373:2425–2437. https://doi.org/10.1056/NEJMoa1509388

Burger, J.A., D.A. Landau, A. Taylor-Weiner, I. Bozic, H. Zhang, K. Sarosiek, L. Wang, C. Stewart, J. Fan, J. Hoellenriegel, et al. 2016. Clonal evolution in patients with chronic lymphocytic leukaemia developing resistance to BTK inhibition. *Nat. Commun.* 7:11589. https://doi.org/10.1038/ncomms11589

Burroughs, J., P. Gupta, B.R. Blazar, and C.M. Verfaillie. 1994. Diffusible factors from the murine cell line M2-10B4 support human in vitro hematopoiesis. *Exp. Hematol.* 22:1095–1101.

Byrd, J.C., R.R. Furman, S.E. Coutre, I.W. Flinn, J.A. Burger, K.A. Blum, B. Grant, J.P. Sharman, M. Coleman, W.G. Wierda, et al. 2013. Targeting BTK with ibrutinib in relapsed chronic lymphocytic leukemia. *N. Engl. J. Med.* 369:32–42. https://doi.org/10.1056/NEJMoa1215637

Chen, S.S., F. Batliwalla, N.E. Holodick, X.J. Yan, S. Yancopoulos, C.M. Croce, T.L. Rothstein, and N. Chiorazzi. 2013. Autoantigen can promote progression to a more aggressive TCL1 leukemia by selecting variants with enhanced B-cell receptor signaling. *Proc. Natl. Acad. Sci. USA*. 110:E1500–E1507. https://doi.org/10.1073/pnas.1300616110

Chiorazzi, N., K.R. Rai, and M. Ferrarini. 2005. Chronic lymphocytic leukemia. *N. Engl. J. Med.* 352:804–815. https://doi.org/10.1056/NEJMra041720

Cui, J., Q. Wang, J. Wang, M. Lv, N. Zhu, Y. Li, J. Feng, B. Shen, and J. Zhang. 2009. Basal c-Jun NH2-terminal protein kinase activity is essential for survival and proliferation of T-cell acute lymphoblastic leukemia cells. *Mol. Cancer Ther.* 8:3214–3222. https://doi.org/10.1158/1535-7163.MCT-09-0408

Davis, R.J. 2000. Signal transduction by the JNK group of MAP kinases. *Cell*. 103:239–252. https://doi.org/10.1016/S0092-8674(00)00116-1

Decker, S., A. Zwick, S.K. Saleem, S. Kissel, A. Rettig, K. Aumann, and C. Dierks. 2019. Optimized xenograft protocol for chronic lymphocytic leukemia results in high engraftment efficiency for all CLL subgroups. *Int. J. Mol. Sci.* 20:6277. https://doi.org/10.3390/ijms20246277

Dühren-von Minden, M., R. Übelhart, D. Schneider, T. Wossning, M.P. Bach, M. Buchner, D. Hofmann, E. Surova, M. Follo, F. Köhler, et al. 2012. Chronic lymphocytic leukaemia is driven by antigen-independent cell-autonomous signalling. *Nature*. 489:309–312. https://doi.org/10.1038/nature11309

Furman, R.R., S. Cheng, P. Lu, M. Setty, A.R. Perez, A. Guo, J. Racchumi, G. Xu, H. Wu, J. Ma, et al. 2014. Ibrutinib resistance in chronic lymphocytic leukemia. *N. Engl. J. Med.* 370:2352–2354. https://doi.org/10.1056/NEJMc1402716

George, B., S.M. Chowdhury, A. Hart, A. Sircar, S.K. Singh, U.K. Nath, M. Mamgain, N.K. Singhal, L. Sehgal, and N. Jain. 2020. Ibrutinib resistance mechanisms and treatment strategies for B-cell lymphomas. *Cancers*. 12:1328. https://doi.org/10.3390/cancers12051328

Ghia, P., and F. Caligaris-Cappio. 2006. The origin of B-cell chronic lymphocytic leukemia. *Semin. Oncol.* 33:150–156. https://doi.org/10.1053/j.seminoncol.2006.01.009

Grassi, E.S., V. Vezzoli, I. Negri, Á. Lábadi, L. Fugazzola, G. Vitale, and L. Persani. 2015. SP600125 has a remarkable anticancer potential against undifferentiated thyroid cancer through selective action on ROCK and p53 pathways. *Oncotarget*. 6:36383–36399. https://doi.org/10.18632/oncotarget.5799

Gutierrez, A. Jr., R.C. Tschumper, X. Wu, T.D. Shanafelt, J. Eckel-Passow, P.M. Huddleston III, S.L. Slager, N.E. Kay, and D.F. Jelinek. 2010. LEF-1 is a prosurvival factor in chronic lymphocytic leukemia and is expressed in the preleukemic state of monoclonal B-cell lymphocytosis. *Blood*. 116:2975–2983. https://doi.org/10.1182/blood-2010-02-269878

Hallek, M., B.D. Cheson, D. Catovsky, F. Caligaris-Cappio, G. Dighiero, H. Döhner, P. Hillmen, M.J. Keating, E. Montserrat, K.R. Rai, et al. 2008. Guidelines for the diagnosis and treatment of chronic lymphocytic leukemia: A report from the international workshop on chronic lymphocytic leukemia updating the national cancer institute-working group 1996 guidelines. *Blood*. 111:5446–5456. https://doi.org/10.1182/blood-2007-06-093906

Hamblin, T.J., Z. Davis, A. Gardiner, D.G. Oscier, and F.K. Stevenson. 1999. Unmutated Ig V(H) genes are associated with a more aggressive form of chronic lymphocytic leukemia. *Blood*. 94:1848–1854. https://doi.org/10.1182/blood.V94.6.1848

Hartman, A.D., A. Wilson-Weekes, A. Suvannasankha, G.S. Burgess, C.A. Phillips, K.J. Hincher, L.D. Cripe, and H.S. Boswell. 2006. Constitutive c-jun N-terminal kinase activity in acute myeloid leukemia derives from Flt3 and affects survival and proliferation. *Exp. Hematol.* 34:1360–1376. https://doi.org/10.1016/j.exphem.2006.05.019

Herishanu, Y., P. Pérez-Galán, D. Liu, A. Biancotto, S. Pittaluga, B. Vire, F. Gibellini, N. Njuguna, E. Lee, L. Stennett, et al. 2011. The lymph node microenvironment promotes B-cell receptor signaling, NF-kappaB activation, and tumor proliferation in chronic lymphocytic leukemia. *Blood*. 117:563–574. https://doi.org/10.1182/blood-2010-05-284984

Herman, S.E., R.Z. Mustafa, J.A. Gyamfi, S. Pittaluga, S. Chang, B. Chang, M. Farooqui, and A. Wiestner. 2014. Ibrutinib inhibits BCR and NF-κB signaling and reduces tumor proliferation in tissue-resident cells of patients with CLL. *Blood*. 123:3286–3295. https://doi.org/10.1182/blood-2014-02-548610

Hervé, M., K. Xu, Y.S. Ng, H. Wardemann, E. Albesiano, B.T. Messmer, N. Chiorazzi, and E. Meffre. 2005. Unmutated and mutated chronic lymphocytic leukemias derive from self-reactive B cell precursors despite expressing different antibody reactivity. *J. Clin. Invest.* 115:1636–1643. https://doi.org/10.1172/JCI24387

Hess, P., G. Pihan, C.L. Sawyers, R.A. Flavell, and R.J. Davis. 2002. Survival signaling mediated by c-Jun NH(2)-terminal kinase in transformed B lymphoblasts. *Nat. Genet.* 32:201–205. https://doi.org/10.1038/ng946

Hibi, M., A. Lin, T. Smeal, A. Minden, and M. Karin. 1993. Identification of an oncoprotein- and UV-responsive protein kinase that binds and potentiates the c-Jun activation domain. *Genes Dev.* 7:2135–2148. https://doi.org/10.1101/gad.7.11.2135

Hirata, Y., A. Sugie, A. Matsuda, S. Matsuda, and S. Koyasu. 2013. TAK1-JNK axis mediates survival signal through Mcl1 stabilization in activated T cells. *J. Immunol.* 190:4621–4626. https://doi.org/10.4049/jimmunol.1202809

Inabe, K., T. Miyawaki, R. Longnecker, H. Matsukura, S. Tsukada, and T. Kurosaki. 2002. Bruton's tyrosine kinase regulates B cell antigen receptor-mediated JNK1 response through Rac1 and phospholipase C-gamma2 activation. *FEBS Lett.* 514:260–262. https://doi.org/10.1016/S0014-5793(02)02375-X

Jain, P., P.A. Thompson, M. Keating, Z. Estrov, A. Ferrajoli, N. Jain, H. Kantarjian, J.A. Burger, S. O'Brien, and W.G. Wierda. 2017. Long-term outcomes for patients with chronic lymphocytic leukemia who

discontinue ibrutinib. *Cancer*. 123:2268–2273. https://doi.org/10.1002/cncr.30596

Jiang, A., A. Craxton, T. Kurosaki, and E.A. Clark. 1998. Different protein tyrosine kinases are required for B cell antigen receptor-mediated activation of extracellular signal-regulated kinase, c-Jun NH2-terminal kinase 1, and p38 mitogen-activated protein kinase. *J. Exp. Med.* 188: 1297–1306. https://doi.org/10.1084/jem.188.7.1297

Kanagal-Shamanna, R., P. Jain, K.P. Patel, M. Routbort, C. Bueso-Ramos, T. Alhalouli, J.D. Khoury, R. Luthra, A. Ferrajoli, M. Keating, et al. 2019. Targeted multigene deep sequencing of Bruton tyrosine kinase inhibitor-resistant chronic lymphocytic leukemia with disease progression and Richter transformation. *Cancer*. 125:559–574. https://doi.org/10.1002/cncr.31831

Kelkel, M., C. Cerella, F. Mack, T. Schneider, C. Jacob, M. Schumacher, M. Dicato, and M. Diederich. 2012. ROS-independent JNK activation and multisite phosphorylation of Bcl-2 link diallyl tetrasulfide-induced mitotic arrest to apoptosis. *Carcinogenesis*. 33:2162–2171. https://doi.org/10.1093/carcin/bgs240

Lampson, B.L., and J.R. Brown. 2018. Are BTK and PLCG2 mutations necessary and sufficient for ibrutinib resistance in chronic lymphocytic leukemia? *Expert Rev. Hematol.* 11:185–194. https://doi.org/10.1080/17474086.2018.1435268

Landau, D.A., S.L. Carter, P. Stojanov, A. McKenna, K. Stevenson, M.S. Lawrence, C. Sougnez, C. Stewart, A. Sivachenko, L. Wang, et al. 2013. Evolution and impact of subclonal mutations in chronic lymphocytic leukemia. *Cell*. 152:714–726. https://doi.org/10.1016/j.cell.2013.01.019

Liebig, T.M., A. Fiedler, S. Zoghi, A. Shimabukuro-Vornhagen and M.S. Von Bergwelt-Baildon. 2009. Generation of human CD40-activated B cells. *J. Vis. Exp.*:1373. https://doi.org/10.3791/1373

Lin, A. 2003. Activation of the JNK signaling pathway: Breaking the brake on apoptosis. *BioEssays*. 25:17–24. https://doi.org/10.1002/bies.10204

Maddocks, K.J., A.S. Ruppert, G. Lozanski, N.A. Heerema, W. Zhao, L. Abruzzo, A. Lozanski, M. Davis, A. Gordon, L.L. Smith, et al. 2015. Etiology of ibrutinib therapy discontinuation and outcomes in patients with chronic lymphocytic leukemia. *JAMA Oncol.* 1:80–87. https://doi.org/10.1001/jamaoncol.2014.218

Minici, C., M. Gounari, R. Übelhart, L. Scarfò, M. Dühren-von Minden, D. Schneider, A. Tasdogan, A. Alkhatib, A. Agathangelidis, S. Ntoufa, et al. 2017. Distinct homotypic B-cell receptor interactions shape the outcome of chronic lymphocytic leukaemia. *Nat. Commun.* 8:15746. https://doi.org/10.1038/ncomms15746

Morabito, F., M. Gentile, J.F. Seymour, and A. Polliack. 2015. Ibrutinib, idelalisib and obinutuzumab for the treatment of patients with chronic lymphocytic leukemia: Three new arrows aiming at the target. *Leuk. Lymphoma*. 56:3250–3256. https://doi.org/10.3109/10428194.2015.1061193

Nagy, M.A., R. Hilgraf, D.S. Mortensen, J. Elsner, S. Norris, J. Tikhe, W. Yoon, D. Paisner, M. Delgado, P. Erdman, et al. 2021. Discovery of the c-jun N-terminal kinase inhibitor CC-90001. *J. Med. Chem.* 64:18193–18208. https://doi.org/10.1021/acs.jmedchem.1c01716

Parra, E. 2012. Inhibition of JNK-1 by small interfering RNA induces apoptotic signaling in PC-3 prostate cancer cells. *Int. J. Mol. Med.* 30:923–930. https://doi.org/10.3892/ijmm.2012.1055

Pepper, C., T.T. Lin, G. Pratt, S. Hewamana, P. Brennan, L. Hiller, R. Hills, R. Ward, J. Starczynski, B. Austen, et al. 2008. Mcl-1 expression has in-vitro and in vivo significance in chronic lymphocytic leukemia and is associated with other poor prognostic markers. *Blood*. 112:3807–3817. https://doi.org/10.1182/blood-2008-05-157131

Petlickovski, A., L. Laurenti, X. Li, S. Marietti, P. Chiusolo, S. Sica, G. Leone, and D.G. Efremov. 2005. Sustained signaling through the B-cell receptor induces Mcl-1 and promotes survival of chronic lymphocytic leukemia B cells. *Blood*. 105:4820–4827. https://doi.org/10.1182/blood-2004-07-2669

Pfeifer, D., M. Pantic, I. Skatulla, J. Rawluk, C. Kreutz, U.M. Martens, P. Fisch, J. Timmer, and H. Veelken. 2007. Genome-wide analysis of DNA copy number changes and LOH in CLL using high-density SNP arrays. *Blood*. 109:1202–1210. https://doi.org/10.1182/blood-2006-07-034256

Popmihajlov, Z., D.J. Sutherland, G.S. Horan, A. Ghosh, D.A. Lynch, P.W. Noble, L. Richeldi, T.F. Reiss, and S. Greenberg. 2022. CC-90001, a c-Jun N-terminal kinase (JNK) inhibitor, in patients with pulmonary fibrosis: Design of a phase 2, randomised, placebo-controlled trial. *BMJ Open Respir. Res.* 9:e001060. https://doi.org/10.1136/bmjresp-2021-001060

Puente, X.S., M. Pinyol, V. Quesada, L. Conde, G.R. Ordóñez, N. Villamor, G. Escaramis, P. Jares, S. Beà, M. González-Díaz, et al. 2011. Whole-genome sequencing identifies recurrent mutations in chronic lymphocytic leukaemia. *Nature*. 475:101–105. https://doi.org/10.1038/nature10113

Raptis, L., and J.B. Bolen. 1989. Polyomavirus transforms rat F111 and mouse NIH 3T3 cells by different mechanisms. *J. Virol.* 63:753–758. https://doi.org/10.1128/jvi.63.2.753-758.1989

Rassenti, L.Z., L. Huynh, T.L. Toy, L. Chen, M.J. Keating, J.G. Gribben, D.S. Neuberg, I.W. Flinn, K.R. Rai, J.C. Byrd, et al. 2004. ZAP-70 compared with immunoglobulin heavy-chain gene mutation status as a predictor of disease progression in chronic lymphocytic leukemia. *N. Engl. J. Med.* 351:893–901. https://doi.org/10.1056/NEJMoa040857

Redondo-Muñoz, J., E. Escobar-Díaz, M. Hernández Del Cerro, A. Pandiella, M.J. Terol, J.A. García-Marco, and A. García-Pardo. 2010. Induction of B-chronic lymphocytic leukemia cell apoptosis by arsenic trioxide involves suppression of the phosphoinositide 3-kinase/Akt survival pathway via c-jun-NH2 terminal kinase activation and PTEN upregulation. *Clin. Cancer Res.* 16:4382–4391. https://doi.org/10.1158/1078-0432.CCR-10-0072

Schneider, C.A., W.S. Rasband, and K.W. Eliceiri. 2012. NIH Image to ImageJ: 25 years of image analysis. *Nat. Methods*. 9:671–675. https://doi.org/10.1038/nmeth.2089

Seliger, B., S. Jasinski-Bergner, C. Massa, A. Mueller, K. Biehl, B. Yang, M. Bachmann, D. Jonigk, P. Eichhorn, A. Hartmann, et al. 2022. Induction of pulmonary HLA-G expression by SARS-CoV-2 infection. *Cell. Mol. Life Sci.* 79:582. https://doi.org/10.1007/s00018-022-04592-9

Valla, K., C.R. Flowers, and J.L. Koff. 2018. Targeting the B cell receptor pathway in non-Hodgkin lymphoma. *Expert Opin. Investig. Drugs*. 27: 513–522. https://doi.org/10.1080/13543784.2018.1482273

van Attekum, M.H.A., J.A.C. van Bruggen, E. Slinger, M.C. Lebre, E. Reinen, S. Kersting, E. Eldering, and A.P. Kater. 2017. CD40 signaling instructs chronic lymphocytic leukemia cells to attract monocytes via the CCR2 axis. *Haematologica*. 102:2069–2076. https://doi.org/10.3324/haematol.2016.157206

Van Gassen, S., B. Callebaut, M.J. Van Helden, B.N. Lambrecht, P. Demeester, T. Dhaene, and Y. Saeys. 2015. FlowSOM: Using self-organizing maps for visualization and interpretation of cytometry data. *Cytometry A*. 87: 636–645. https://doi.org/10.1002/cyto.a.22625

Vanni, F., L. Lopresti, V. Zurli, A. Kabanova, F. Cattaneo, A. Sicuranza, A. Gozzetti, S. Gemma, D.M. Zisterer, M. Bocchia, et al. 2021. A novel class of oxazepine-based anti-cancer agents induces cell death in primary human CLL cells and efficiently reduces tumor growth in Eμ-TCL1 mice through the JNK/STAT4/p66Shc axis. *Pharmacol. Res.* 174:105965. https://doi.org/10.1016/j.phrs.2021.105965

Vargova, K., N. Curik, P. Burda, P. Basova, V. Kulvait, V. Pospisil, F. Savvulidi, J. Kokavec, E. Necas, A. Berkova, et al. 2011. MYB transcriptionally regulates the miR-155 host gene in chronic lymphocytic leukemia. *Blood*. 117:3816–3825. https://doi.org/10.1182/blood-2010-05-285064

Vivas-Mejia, P., J.M. Benito, A. Fernandez, H.D. Han, L. Mangala, C. Rodriguez-Aguayo, A. Chavez-Reyes, Y.G. Lin, M.S. Carey, A.M. Nick, et al. 2010. c-Jun-NH2-kinase-1 inhibition leads to antitumor activity in ovarian cancer. *Clin. Cancer Res.* 16:184–194. https://doi.org/10.1158/1078-0432.CCR-09-1180

Wei, Y., S. Pattingre, S. Sinha, M. Bassik, and B. Levine. 2008a. JNK1-mediated phosphorylation of Bcl-2 regulates starvation-induced autophagy. *Mol. Cell*. 30:678–688. https://doi.org/10.1016/j.molcel.2008.06.001

Wei, Y., S. Sinha, and B. Levine. 2008b. Dual role of JNK1-mediated phosphorylation of Bcl-2 in autophagy and apoptosis regulation. *Autophagy*. 4:949–951. https://doi.org/10.4161/auto.6788

Weston, C.R., and R.J. Davis. 2007. The JNK signal transduction pathway. *Curr. Opin. Cell Biol.* 19:142–149. https://doi.org/10.1016/j.ceb.2007.02.001

Wiestner, A., A. Rosenwald, T.S. Barry, G. Wright, R.E. Davis, S.E. Henrickson, H. Zhao, R.E. Ibbotson, J.A. Orchard, Z. Davis, et al. 2003. ZAP-70 expression identifies a chronic lymphocytic leukemia subtype with unmutated immunoglobulin genes, inferior clinical outcome, and distinct gene expression profile. *Blood*. 101:4944–4951. https://doi.org/10.1182/blood-2002-10-3306

Woyach, J.A., R.R. Furman, T.M. Liu, H.G. Ozer, M. Zapatka, A.S. Ruppert, L. Xue, D.H. Li, S.M. Steggerda, M. Versele, et al. 2014. Resistance mechanisms for the Bruton's tyrosine kinase inhibitor ibrutinib. *N. Engl. J. Med.* 370:2286–2294. https://doi.org/10.1056/NEJMoa1400029

Ye, Y., A. Gaudy, M. Thomas, J. Reyes, B. Burkhardt, G. Horan, L. Liu, J. Chen, A. Ghosh, L.N. Carayannopoulos, et al. 2022. Safety, pharmacokinetics, and pharmacodynamics of CC-90001 (BMS-986360), a c-Jun N-terminal kinase inhibitor, in phase 1 studies in healthy participants. *Clin. Pharmacol. Drug Dev.* 11:1394–1404. https://doi.org/10.1002/cpdd.1178

Yu, C., Y. Minemoto, J. Zhang, J. Liu, F. Tang, T.N. Bui, J. Xiang, and A. Lin. 2004. JNK suppresses apoptosis via phosphorylation of the proapoptotic Bcl-2 family protein BAD. *Mol. Cell*. 13:329–340. https://doi.org/10.1016/S1097-2765(04)00028-0

Supplemental material

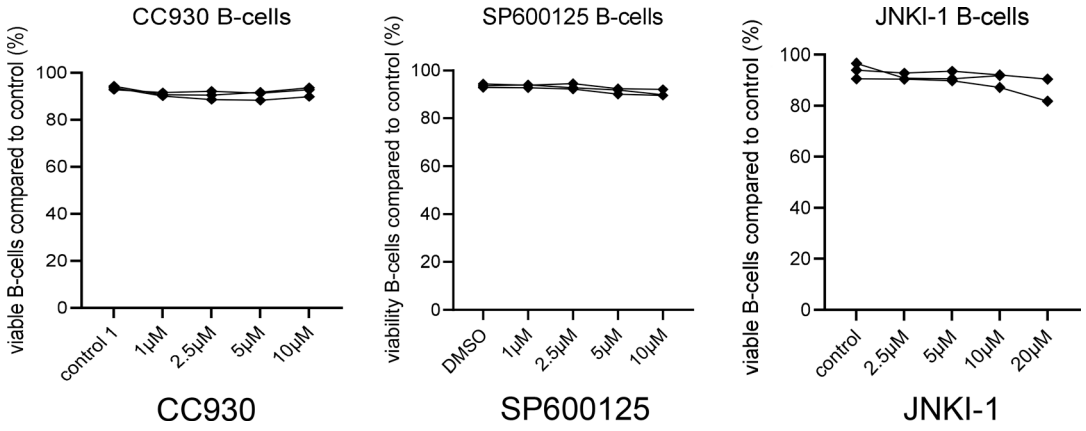

Figure S1. **Relative viability of B cells extracted from the PB of healthy donors and treated with different concentrations of JNK1 inhibitors or controls.** Inhibitors used were CC930, SP600125, and L-JNKi at the indicated concentrations, and viability was assessed by Annexin V/7-AAD staining. Results for each concentration were compared with the DMSO control.

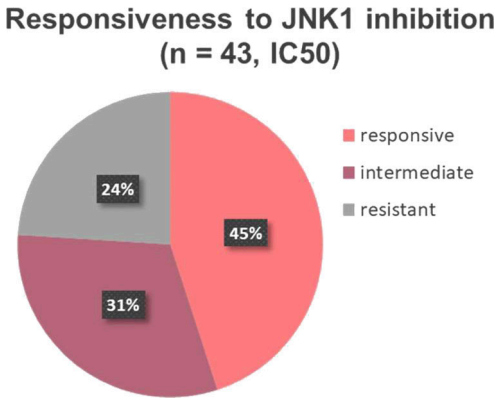

Figure S2. **Distribution of response groups of CLL cells treated with the three different JNK1 inhibitors SP600125 CC-930 or the peptide inhibitor L-JNKi.** Sensitivity to the inhibitors was defined as IC50 below 2 µM to the kinase inhibitors and below 3 µM to the peptide inhibitor JNK1i. In the responsive group, the CLL sample was sensitive to all three inhibitors, in the intermediate responsive group the CLL sample was sensitive to 1–2 inhibitors, and in the resistant group, the CLL sample did not respond to any JNK1 inhibitor. IC50 values were determined after 24 h of inhibitor treatment.

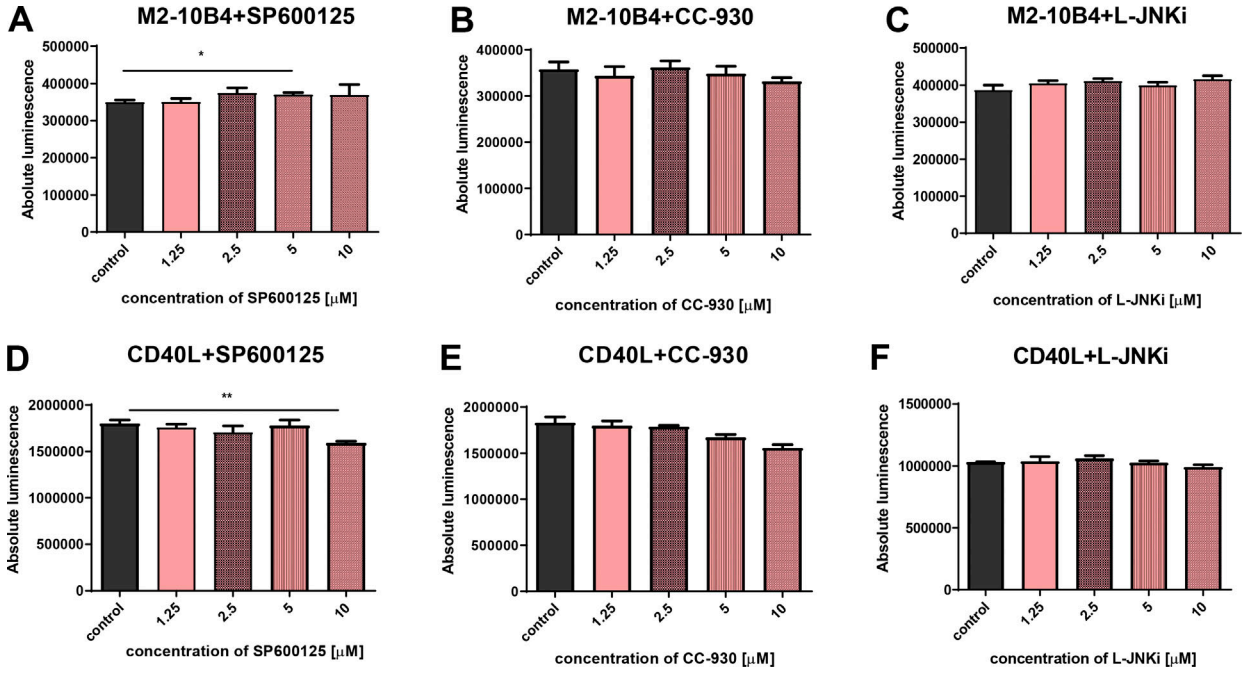

Figure S3. **Treatment of stroma cells with JNIK1 inhibitors. (A–C)** CellTiter-Glo assay of M2-10B4 stromal cells after 24 h of treatment with SP600125 (left), CC-930 (middle), and L-JNKi (right) inhibitors. **(D–F)** CellTiter-Glo assay of CD40L secreting cells after 24 h of treatment with SP600125 (left), CC-930 (middle), and L-JNKi (right) inhibitors (unpaired *t* test, *P < 0.05).

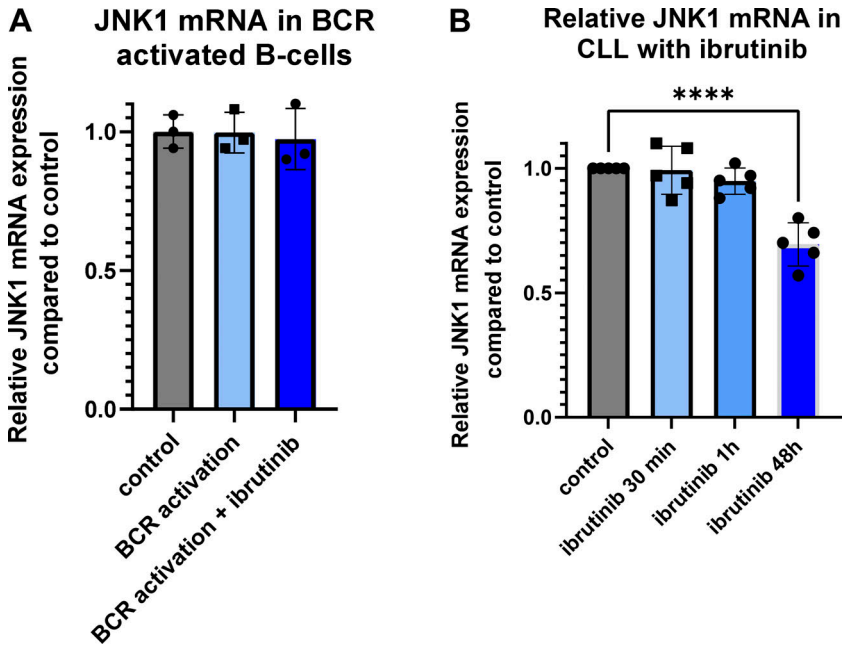

Figure S4. **JNK1 mRNA expression after ibrutinib treatment. (A)** B cells from healthy donors were isolated and stimulated with anti-IgM antibody to induce BCR activation for 1 h with and without ibrutinib treatment (2 μM). BCR activity was assessed via intracellular BTK phosphorylation. JNK1 mRNA levels were detected via TaqMan PCR and normalized to GAPDH (see Materials and methods section). The graph shows relative JNK1 transcript levels for three different blood donors. **(B)** CLL cells (*n* = 5 pts) were treated with ibrutinib 2 μM for 0.5, 1, and 48 h, and relative mRNA levels for JNK1 were assessed as described above. Controls were set to 1 for each individual patient (unpaired *t* test, ****P < 0.0001).

Provided online are Table S1, Table S2, and Table S3. Table S1 describes CLL patient samples including response of individual patients to different treatments. Table S2 shows individual JNK1 protein and RNA expression. Table S3 lists antibodies.